C.P. No. 889

MINISTRY OF AVIATION

AERONAUTICAL RESEARCH COUNCIL

CURRENT PAPERS

Some Exploratory Tests on a Two-Dimensional Blown-Cylinder Model in the R.A.E. 2ft x 1½ft Transonic Wind Tunnel

by

A. F. Jones and W. R. Buckingham

LONDON: HER MAJESTY'S STATIONERY OFFICE

1967

SEVEN SHILLINGS NET

U.D.C. No. 533.696.3:533.694.2:533.6.011.7:533.6.048.2:533.6.011.32

C.P. No. 889
December 1964

SOME EXPLORATORY TESTS ON A TWO-DIMENSIONAL BLOWN-CYLINDER MODEL IN THE R.A.E. 2 FT × 1½ FT TRANSONIC-WIND TUNNEL

by

A. F. Jones

W. R. Buckingham

SUMMARY

Static pressure measurements have been made at subsonic Mach numbers to examine compressibility effects on a two-dimensional circular cylinder with two tangential blowing slots. These results together with forces derived from them are briefly discussed.

Replaces R.A.E. Tech. Report No. 64090 - A.R.C. 26850.

CONTENTS

1 INTRODUCTION

A type of helicopter has been suggested[1] which converts after take-off to a conventional aircraft configuration by means of retractable rotor-blades. Two features of such a rotor are that the section be structurally stiff, and also possess a very small lift-curve slope while the rotor is stopped for the retraction operation. At the same time, a reasonable lift/drag ratio is required of the rotor when in the lifting configuration. It has been suggested[1] that a circular section with circulation control by blowing through tangential slots might be a suitable section for such a machine.

Some initial tests on two-dimensional sections were conducted at N.G.T.E. and N.P.L.[2]. Various experimental difficulties were encountered, but it was demonstrated that large lifting forces can be attained at low speeds albeit with a substantial drag penalty. Furthermore, regions of locally supersonic flow could be produced even at very low forward speeds. The present tests were initiated by N.G.T.E. with the object of extending related work to moderate subsonic Mach numbers (as might be expected on the outer sections of a rotor) in view of the compressibility effects already encountered at low speeds. The work reported here was undertaken as part of an initial investigation in view of the novelty of the configuration, and not as a complete programme. The results obtained go some way toward achieving the objective, but some doubt in the measurements arises due to the appearance of a certain type of wake instability as Mach number is increased. It is shown that the locus defining the onset of this instability may depend to some extent on the test conditions, so that confirmation from tests in a different (and preferably much larger) wind tunnel would be desirable.

2 MODEL AND TEST FACILITY

The R.A.E. 2 ft × 1½ ft transonic wind tunnel is a continuous, closed circuit facility[3] with a slotted wall test section utilising effuser suction to generate transonic and supersonic Mach numbers. The working section and effuser are enclosed in a large plenum chamber. The free-stream Mach number is continuously variable from 0.42 up to 1.30 with two lower Mach numbers, 0.16 and 0.30, obtainable by fixed settings of a throttling valve downstream of the effuser. The total pressure may be varied in the range 5" to 30" Hg absolute, dependent on the Mach number.

In these tests, only the tunnel roof and floor were slotted, each having six tapered slots giving an overall open area ratio of 6%. The side walls

were of unslotted glass, and acted as end-plates while allowing the use of a conventional schlieren system. The model was built in three equal length sections, and spanned the major dimension of the working section, passing through the side walls to vertical supports. The general arrangement is shown in Fig. 1. One section forms a completely separate "dummy" section cantilevered from one side. The remaining pair form a "live" and an "earth" section and were joined through a hollow cylindrical tube originally intended to form the flexure for a strain-gauge balance. This assembly was then cantilevered via the "earth" section from the opposite side of the tunnel. A minimum gap was maintained between the "live" and "dummy" sections. Static pressure tappings were distributed at equal angular intervals (of 20°) around the circumference at spanwise stations in the centre of each section. Further points in the plenum chamber of each slot recorded the jet total pressures at each spanwise station. The jet air was supplied along ducts co-axial with the balance, a single duct supplying both slots in a particular section. Air for the "earth" section was distributed through an annulus surrounding the duct which supplied the "live" section. An arrangement of gauzes, grooves and internal slots was employed in an effort to maintain a uniform spanwise total pressure distribution close to the ends of each section.

The slot geometry (Fig.1) was that favoured by the N.G.T.E. at the time the model was designed. The slots were 60° apart and the primary slot had twice the throat height of the secondary slot. The entire assembly could be rotated to any attitude (Fig.1) in the range $-5^{\circ} < \sigma < 50^{\circ}$ but was fixed for any particular run.

Dry air was drawn from the tunnel circuit and returned via a drier to the slots after compression by a single cylinder reciprocating compressor[4]. The oil filters and anti-pulsators currently being added to this system were not available for these tests so that the jet air contained a small amount of oil vapour and fluctuated slightly in pressure with a frequency related to the compressor speed of 330 rpm. The mass flow supplied to each section (but not the individual slots) was controllable, and was measured using standard orifice plate assemblies[5]. The model design was developed by T.E.M. (Engineering) Ltd under the supervision of Mr. J. E. Johnson of the R.A.E.

3 EXPERIMENTAL TECHNIQUE

The total pressure losses in the ducting to the three sections differed substantially, and these losses were balanced by additional resistance so as

to allow the three sets of orifice pressures to be recorded on an alcohol multi-manometer, relative to a datum pressure which, together with the slot total pressures was recorded on a mercury multi-manometer. Calibration of the slots for spanwise uniformity proved to be a difficult problem due to the small slot heights involved (0.010" and 0.020" respectively). In an attempt to obtain a crude qualitative assessment, a rectangular total-pressure probe was used, with the major dimension normal to the plane of the jet and large enough to assure interception of all the jet flow at any spanwise station. A single jet pressure ratio was chosen, large enough to ensure sonic flow at the slot exit. Traverses at zero free stream velocity with this probe showed localised falls in total pressure at the junctions between the three sections, together with a roughly constant spanwise gradient across each section.

The static pressure measurements on the model were made using automatic capsule manometers[6] with a range of one atmosphere and a nominal accuracy of ± 0.2 lb/ft^2 using an upstream total pressure measurement as a reference. Due to the long tubes involved in this system, the response time of these instruments is very long so that all pressure distributions are time-average values. The static pressures on the centre-line of the tunnel roof and floor were also recorded during some tests using alcohol multi-manometers of nominal accuracy ± 0.01" alcohol with the tunnel static pressure as a reference.

As described in section 2, the tube joining the "live" and "earth" sections was originally intended to form the flexure for a three component strain-gauge balance. However this proved to be unsatisfactory. Consequently for these tests the static pressure distributions were integrated numerically to give force coefficients C_z' and C_x' (in body axes), with no allowance for skin friction. The large angular interval between the static pressure tappings inevitably reduces the accuracy of this process. The overall forces (excluding friction) are obtained by adding the resolved components of the jet momentum to the integrated static pressures. Thus, for the present configuration, approximately:-

$$C_z = C_z' - \frac{1}{2\sqrt{3}} C_\mu \qquad (1)$$

$$C_x = C_x' + \frac{5}{6} C_\mu \qquad (2)$$

As discussed in section 4.1, no tunnel interference corrections were applied to the force coefficients presented in this Report.

Procedure during a test at a given incidence consisted of varying the total pressure of the jet at constant Mach number and total pressure of the free-stream. The jet total pressures in each of the three sections of the model were controlled to a common value for each data point. This method appears to give fairly good agreement between the static pressure distributions at the three spanwise stations (Fig.4) in spite of the flow non-uniformities noted above.

3.1 Range of test parameters

The number of controllable parameters is embarrassingly large, and an appropriate choice poses a major problem. The variables are free-stream Mach number and Reynolds number, slot orientation σ, and either $C\mu$ or slot pressure ratio P_j/p_∞. Previous work[2] suggested that slot orientation was not a major parameter so that, since this was an initial investigation, σ was kept constant at 0° for all tests. The basic requirement is clearly for variation of $C\mu$ (or P_j/p_∞), and Mach number, at constant Reynolds number.

Choice of the appropriate Reynolds number is complicated by the fact that the critical Reynolds number range for the symmetric flow past an unblown circular cylinder (2.5 to 4×10^5) [11] cannot be exceeded with the present model and tunnel for Mach numbers below 0.55. However, there is evidence[12] that the significance of this Reynolds number range decreases with increasing Mach number, and even at low Mach numbers its relevance to the lifting configuration is not obvious. In an attempt to reduce the sensitivity of the flow to Reynolds number at low speeds, bands of distributed roughness (carborundum) were applied ahead of $\theta = 80^\circ$ to promote early transition, and thus prevent boundary layer separation ahead of $\theta = 90^\circ$. However even quite large grain sizes, (relative to model diameter) produced only minor changes in the pressure distribution corresponding to small changes in the separation position. All tests were therefore completed without roughness, and in most cases at a Reynolds number ($\approx 1.8 \times 10^5$) somewhat below the critical value, in an attempt to obviate (at least for small lift) complications arising due to changes from a laminar to a turbulent type of separation.

As regards the appropriate blowing parameter, it is not established whether $C\mu$ or P_j/p_∞ is the primary variable. The present experiment can do

little to resolve this since when the slots are choked, the two parameters are not independent but are related through the slot geometry. Also, the range of $C\mu$ in the test is limited by its dependence on free-stream Mach number (Fig.2).

4 DISCUSSION OF RESULTS

4.1 Tunnel constraint effects

The conventional linearised theory methods for estimating constraint effects are not applicable in this case because the section is very thick, and also because the flow is not attached to a large part of the model surface, thus producing a wide wake. In Ref.13, a method has been developed to deal with the effects of large wakes, but only in the case where the separation points are well defined and independent of the constraint. The slotted roof and floor constitute an additional complication to the problem although they may be expected to reduce the magnitude of the blockage corrections.

For these reasons all data in this report are presented without correction. The most serious objection to this procedure arises for the very high values of C_z' obtained at the lower speeds, since even the linear theory[8] contribution to the downwash at the model ($\approx 1.3\ c_z'$) becomes very large.* Resolution into lift and drag axes therefore becomes an uncertain process for large C_z'.

4.2 Low speed results

A feature of the results both at $M_\infty = 0.16$ (Fig.5) and 0.3 (Fig.7) is an asymmetric pressure distribution leading to a non-zero C_z' (Figs.14 and 15) at $C\mu = 0$. This arises since the slots are supplied from a common duct so that some venting occurs with the jet nominally "off". Apart from this asymmetry, the distributions are similar to the symmetric flow past an unblown cylinder at a high sub-critical Reynolds number, with laminar separations probably occurring ahead of $\theta = 90^\circ$ and 270°, followed by a region in which the pressure is approximately constant.** The immediate effect of a non-zero value of $C\mu$ is a rearward shift of the separation point on the upper surface

---

* This value should be compared with the tentative recommendation in Ref.9, that lift constraint corrections be kept below a maximum of 2°.

** This pressure is hereafter referred to as the base pressure.

(probably to a point between the two slots), thus producing a pressure distribution on that side which is similar to that of a symmetrical inviscid flow, and also raising the base pressure. The important point here is that a large part of the lift and some of the drag reduction arises from the forward influence from the slot at $\theta = 90^{\circ}$. Increasing $C\mu$ results in a movement of the probable separation position to a point beyond the second slot, giving further increases in base pressure and a rapid increase of the peak suction. As $C\mu$ is further increased, the peak suction continues to rise and at $M_{\infty} = 0.30$ a region exists where the local Mach number on the surface, derived from p/P_{∞}, substantially exceeds unity. Subsequently, at $M_{\infty} = 0.30$, a peak also appears aft of the secondary slot and a second supersonic region develops, while at $M_{\infty} = 0.16$ a secondary peak appears likely for even higher $C\mu$. The base pressure now varies only slowly with $C\mu$, and if the extent of the constant-pressure region gives any guide, the separation points are also varying slowly with a possible forward movement on the pressure side. Dunham[14] has proposed a simple theoretical model for a type of flow similar to the present one for low Mach numbers and relatively large values of C_z' (> 5, say). The pressure distribution is represented on the upstream side of the cylinder by that for an inviscid flow with circulation, and in the separated region by a constant pressure equal to the experimentally observed base pressure. This semi-empirical distribution is then rotated around the cylinder until the theoretical and experimental stagnation points coincide, and the circulation is chosen so that the lift corresponding to the theoretical pressure distribution is equal to the resolved component of the measured force. This model is a fair representation also of the present results (Fig.6) at $M_{\infty} = 0.16$ for $C_z' < 9$ approximately; above this value, there is some difficulty in obtaining convergence in the iterative process for determining the circulation.

The experimental pressure distributions have been integrated to give force coefficients (in body axes) shown in Figs.14 and 15. These show an initial fall in the value of C_x' due to the increased base pressure and the high suctions developed on the upstream side of the cylinder, and a rapid and very roughly linear increase in C_z'. At both Mach numbers, the slope of the $C_z' \sim C\mu$ curve is significantly reduced for the high $C\mu$ values for which the separation points and base pressures appear to vary only slowly. Thus further increase in C_z' is obtained by increases in the peak suction only,

rather than by both this and simultaneous increases in the projected area over which the suction acts, as at lower $C\mu$. The increase in C'_x arises in spite of the increasing base pressure because of the high suctions aft of $\theta = 90^\circ$. The results at $M_\infty = 0.30$ show no sensitivity to small variations in Reynolds number.

4.3 Compressibility effects

The pressure distributions in Figs.5, 7 and 8 show that there is a strong compressibility effect. In particular, the critical value of the pressure coefficient, C_p^*, is exceeded and local supersonic regions appear when the blowing rate and when the Mach number are sufficiently increased. There is thus an initial increase of the normal force with free-stream Mach number, for constant values of $C\mu$, as is to be expected for subcritical flows. This is shown in Fig.17(b). There are not enough experimental points to allow a more detailed analysis, but a line is shown beyond which the flow is locally supersonic. This occurs initially downstream of the first slot. The critical line lies close to that calculated[10] for the inviscid circulatory flow past a circular cylinder with the same normal force. The latter values may, therefore, be used to obtain a rough estimate of the critical Mach number. The most drastic change which occurs as the Mach number is increased beyond the critical value is the sharp fall of the normal force curve.

In the supercritical flow regime, two distinct wake configurations appear, depending on P_j/p_∞ (or $C\mu$). These are:-

(a) For P_j/p_∞ below some critical value at a given Mach number, there is large-scale periodic vortex shedding, as observed under certain conditions in symmetric flow past a circular cylinder at high subcritical Reynolds numbers and low Mach numbers. However, at supercritical Mach numbers, the intensity of the vortex shedding increases, and is accompanied by shock movements on the surface and in the wake. Some spark schlieren photographs (Fig.10(b)) give an indication of the length scales of the periodicity in the wake (denoted type "A") compared with the cylinder diameter. Shock waves (of unknown strength) were readily observed to be moving rapidly upstream, apparently originating in the wake. The photographs (taken at random time intervals) have been arranged in sequence to conform with this motion.

(b) For P_j/p_∞ above the critical value, the alternative wake configuration appears (Fig.10(a)), in which, though the wake is still large compared

with the cylinder diameter and is possibly still periodic, the gross fluctuations of the type "A" configuration are no longer in evidence. This alternative regime (Fig.10(a)) denoted type "B", more closely resembles the flow pattern observed in the wake of a non-lifting unblown cylinder, with turbulent separations as at supercritical Reynolds numbers and low Mach numbers.

At Mach numbers above 0.5 the transition between these two regimes becomes increasingly abrupt and occurs at values of P_j/p_∞ which increase rapidly with Mach number. There is some unsteadiness and hysteresis at the transition, but the mean pressures (e.g. Fig.11) show the major change to be an increase in base pressure giving rise to a sharp change in C'_z and C'_x. The critical values of P_j/p_∞ have been found approximately (Fig.9) for subcritical ($< 2 \times 10^5$) and also for supercritical ($>4 \times 10^5$) Reynolds numbers, where the results are similar but the values of $(P_j/p_\infty)_{crit}$ are somewhat lower at each Mach number. Static pressure measurements on the slotted roof and floor suggested the possibility of some upstream influence (Fig.12) from the diffuser, which might conceivably provide a triggering mechanism. The model was therefore moved seven diameters upstream (Fig.13) and although the overall behaviour is similar, the values of $(P_j/p_\infty)_{crit}$ are somewhat lower in each case (Fig.9). The forward model position is rather extreme, and the influence of the model on the roof and floor pressures (Fig.13) extends into the contraction so that the free-stream Mach number does not reach the nominal undisturbed value upstream of the model. The effective free-stream Mach numbers may, therefore, be lower than the nominal values used here, thus reducing the difference between the two sets of curves. However, this discrepancy is not completely resolved. All measurements discussed below were obtained with the model in the downstream position as in Fig.12.

The pressure distributions and derived force curves are shown in Figs.8 and 16. From the pressures it is clear that only up to $M_\infty = 0.5$ is there any significant development of pressures approaching those for a symmetric inviscid flow ahead of the slot at 90°. Since this was the primary mechanism of lift development for small $C\mu$ at low-speeds, it is perhaps not surprising to find that no worthwhile lifting capability was obtained above this Mach number. The experimental values for C'_z in Fig.17 show the adverse effects of supercritical Mach numbers for constant P_j/p_∞ and also for

constant $C\mu$. For a given $C\mu$, C_z' has a maximum value at a particular free-stream Mach number and falls rapidly thereafter.

Finally, it should be noted that, for Mach numbers above 0.5, no measurements could be obtained above $(P_j/p_\infty)_{crit}$ as discussed above. Since there is a suggestion that this phenomenon may be dependent on the test conditions, these results must be regarded as tentative.

5 CONCLUSIONS

Static pressure measurements have been made at subsonic Mach numbers to examine compressibility effects on a two-dimensional circular cylinder with two tangential blowing slots. The pressure distributions have been integrated to give the corresponding force coefficients without correction for possible tunnel constraint effects.

At low free-stream Mach numbers high normal force coefficients are obtained but the wake remains wide, leading to a large axial force coefficient. Small increases in Mach number are accompanied by comparatively large compressibility effects. Local supersonic regions begin to appear at a critical Mach number which lies fairly close to that calculated for the inviscid circulatory flow with the same normal force. For constant $C\mu$, C_z' increases at first with Mach number, but then falls rapidly as the Mach number is increased beyond the critical value. Under the test conditions, two distinct types of flow are possible in the wake, depending on P_j/p_∞ or $C\mu$; one of them is highly unsteady. The boundary between these two regimes may be influenced by changes in the test environment. Another (and preferably very much larger) facility would be needed if these effects were to be elucidated further.

Appendix A

DERIVATION OF THE JET MOMENTUM COEFFICIENT C_μ

Following Ref.7 we define:-

$$C_\mu = \frac{m_j v_j}{q_\infty Sg}, \qquad A\ (1)$$

where suffix ∞ denotes the undisturbed free-stream conditions, and v_j is the velocity that would be attained by isentropic expansion of the jet air to p_∞. Thus $m_j v_j$ represents the maximum momentum which could be obtained from the jet air for use say as thrust or lift. For adiabatic flow the energy equation gives:-

$$\frac{\gamma}{\gamma - 1} \cdot \frac{p_\infty}{\rho_\infty} + \frac{1}{2} v_j^2 = \frac{\gamma}{\gamma - 1} \frac{P_j}{\rho_j} \qquad A\ (2)$$

where P_j and ρ_j are the stagnation values for the jet. For isentropic flow (2) gives:-

$$v_j = \left\{ \frac{2\gamma R}{(\gamma - 1)} T_j \left[1 - \left(\frac{p_\infty}{P_j} \right)^{\frac{\gamma - 1}{\gamma}} \right] \right\}^{\frac{1}{2}}. \qquad A\ (3)$$

For the orifice plate measurement of mass flow Ref.5 gives:-

$$m = C \left[\frac{h P_{oj}}{T_{oj}} \right]^{\frac{1}{2}}, \qquad A\ (4)$$

where C is a constant dependent on orifice geometry, h is the differential pressure across the orifice plate and P_{oj}, T_{oj} are the stagnation pressure and temperature just upstream of it. In the present case we have two jets so that:-

$$C_\mu = \frac{m_1 v_{j1}}{q_\infty Sg} + \frac{m_2 v_{j2}}{q_\infty Sg}$$

$$= \frac{m_1 v_{j1}}{q_\infty Sg} \left[1 + \frac{m_2 v_{j2}}{m_1 v_{j1}} \right] \qquad A\ (5)$$

If the flow through the two jets is choked we may write:-

$$m = \rho^* A^* v^*$$
$$\propto A^* P T^{-\frac{1}{2}}.$$

Hence

$$\frac{m_1}{m_2} = \frac{A_1^*}{A_2^*} \cdot \frac{P_{j1}}{P_{j2}} \cdot \frac{T_{j2}^{\frac{1}{2}}}{T_{j1}^{\frac{1}{2}}}$$

where * denotes value appropriate to local sonic conditions. Now in the present case $T_{j1} = T_{j2}$ so:-

$$\frac{m_1}{m_2} = \frac{A_1^*}{A_2^*} \cdot \frac{P_{j1}}{P_{j2}} . \qquad A\ (6)$$

Thus from (3) and (6), (5) becomes:-

$$C\mu = \frac{m_1 v_{j1}}{q_\infty Sg} \left\{ 1 + \frac{A_2^*}{A_1^*} \cdot \frac{P_{j2}}{P_{j1}} \cdot \frac{\left[1 - \left(\frac{P_\infty}{P_{j2}} \right)^{\frac{\gamma-1}{\gamma}} \right]^{\frac{1}{2}}}{\left[1 - \left(\frac{P_\infty}{P_{j1}} \right)^{\frac{\gamma-1}{\gamma}} \right]^{\frac{1}{2}}} \right\} \qquad A\ (7)$$

Also, from (4):-

$$m_1 + m_2 = C \left[\frac{h P_{oj}}{T_{oj}} \right]^{\frac{1}{2}}$$

and therefore,

$$m_1 \left[1 + \frac{A_2^*}{A_1^*} \cdot \frac{P_{j2}}{P_{j1}} \right] = C \left[\frac{h P_{oj}}{T_{oj}} \right]^{\frac{1}{2}} . \qquad A\ (8)$$

Now the orifice plates are situated close to the model and coupled by heavily insulated hoses. In addition the jet total temperature T_j close to room temperature, so that negligible error is introduced by neglecting the error between it and T_{oj} the total temperature at the orifice plate. (The result is not highly sensitive to errors in this assumption.) Finally using this and (3) together with (8) gives:-

$$m_1 v_{j1} = \frac{C[h P_{oj}]^{\frac{1}{2}}}{\left[1 + \frac{A_2^*}{A_1^*} \cdot \frac{P_{j2}}{P_{j1}}\right]} \left\{ \frac{2\gamma R}{\gamma - 1} \left[1 - \left(\frac{p_\infty}{P_{j1}}\right)^{\frac{\gamma-1}{\gamma}}\right]\right\}^{\frac{1}{2}} \quad A\ (9)$$

Now in order to derive this result we have assumed the flow through the two slots to be choked, as it will be for most subsonic values of p_∞/P_j, since the jets will remain choked as long as the local static pressure just outside the slot is low enough to give at least the sonic pressure ratio across the slot. In the cases where this requirement is not met, the static pressure at the slot exit will be equal to the local static pressure just outside the slot. It seems likely that in such a case this static pressure will not be significantly different from p_∞, and if this difference is small compared with $P_j - p_\infty$ then it is reasonable to write:-

$$m = \rho_t A_t v_t$$

and then assumed $p_t = p_\infty$ so that $v_t = v_j$ and equation (7) then becomes:-

$$C_\mu = \frac{m_1 v_{j1}}{q_\infty S_g} \left\{ 1 + \frac{A_2}{A_1} \left(\frac{P_{j2}}{P_{j1}}\right)^{\frac{\gamma+1}{\gamma}} \frac{\left[1 - \left(\frac{p_\infty}{P_{j2}}\right)^{\frac{\gamma-1}{\gamma}}\right]}{\left[1 - \left(\frac{p_\infty}{P_{j1}}\right)^{\frac{\gamma-1}{\gamma}}\right]} \right\} ; \quad A\ (7a)$$

similarly equation (9) becomes

$$m_1 v_{j1} = \frac{C\left[h P_{oj}\right]^{\frac{1}{2}} \left\{ \frac{2\gamma R}{\gamma - 1} \left[1 - \left(\frac{p_\infty}{P_{j1}}\right)^{\frac{\gamma-1}{\gamma}}\right]\right\}^{\frac{1}{2}}}{\left\{ 1 + \frac{A_2}{A_1} \cdot \frac{P_{j2}}{P_{j1}} \frac{\left[1 - \left(\frac{p_\infty}{P_{j1}}\right)^{\frac{\gamma-1}{\gamma}}\right]}{\left[1 - \left(\frac{p_\infty}{P_{j2}}\right)^{\frac{\gamma-1}{\gamma}}\right]} \right\}} \quad A\ (9a)$$

SYMBOLS

A	cross-sectional area
C	constant in mass flow calibration of orifice plate
C_p	pressure coefficient $= \frac{p - p_\infty}{q_\infty}$
C_x	axial force coefficient $= X/q_\infty S$
C'_x	axial force coefficient $= X'/q_\infty S$
C_z	normal force coefficient $= Z/q_\infty S$
C'_z	normal force coefficient $= Z'/q_\infty S$
C_μ	jet momentum coefficient $= mv_j/q_\infty Sg$
g	acceleration due to gravity
h	pressure difference across orifice plate
M	Mach number
m	mass flow, lb/sec
P	stagnation pressure
p	static pressure
q	kinetic pressure
R	gas constant
Re	Reynolds number based on cylinder diameter
S	reference area = diameter × unit length
v	velocity
x	axial distance
X	axial force (Fig.1(a))
X'	static pressure component of axial force $= \int_0^{2\pi} C_p \cos\theta \, d\theta$
Z	normal force (Fig.1(a))
Z'	static pressure component of normal force $= \int_0^{2\pi} C_p \sin\theta \, d\theta$
γ	ratio of specific heats of a gas
ε	downwash due to lift constraint
θ	angular co-ordinate
ρ	density
ϱ	stagnation density
σ	slot orientation

Suffices

∞	quantity appropriate to undisturbed free-stream condition
1	quantity appropriate to slot at $\theta = 90°$
2	quantity appropriate to slot at $\theta = 150°$
j	quantity appropriate to a jet
t	quantity evaluated at an unchoked throat
* (Affix)	quantity appropriate to local sonic conditions

REFERENCES

No.	Author	Title, etc
1	I.C. Cheeseman	Unpublished M.O.A. Report.
2	Staff of N.G.T.E.	Unpublished M.O.A. Report.
3	D.A. Spence A.S. Bennett	Model tests on an effuser induction scheme for operating a transonic wind tunnel. A.R.C. CP.420, June 1957
4	A.G. Kurn	A base pressure investigation at transonic speeds on an afterbody containing four sonic nozzles and a cylindrical afterbody containing a central sonic nozzle. R.A.E. Tech. Note Aero 2869 (A.R.C.24932) February 1963
5	British Standards Institute	Flow measurement. B.S. 1042
6	G.F. Midwood R.W. Hayward	An automatic self-balancing capsule manometer. A.R.C. CP.231, July 1955
7	A. Anscombe J. Williams	Some comments on high lift testing in wind tunnels with particular reference to jet-blowing models. A.R.C. 18664
8	D.D. Davis, Jun. D. Moore	Analytical study of blockage- and lift-interference for slotted tunnels obtained by the substitution of an equivalent homogeneous boundary for the discrete slots. NACA TIB/3792. NACA RM L53E07b, June 1953
9	S.F.J. Butler J. Williams	Further comments on high-lift testing in wind tunnels with particular reference to jet-blowing models. Aero Quarterly Vol.XI, pp.285-308, August 1960
10	L. Bers	On the circulatory flow of a compressible fluid past a circular cylinder. NACA TN 970, July 1945
11	H. Schlichting	Boundary layer theory. Pergamon Press Ltd. 1955

REFERENCES (CONTD.)

No.	Author	Title, etc
12	L. Howarth (Ed.)	Modern development in fluid dynamics: high speed flow. Vol. II pp 682-686 Oxford Univ. Press 1953
13	E.C. Maskell	A theory of the blockage effects on bluff bodies and stalled wings in a closed wind tunnel. A.R.C. R & M 3400, November 1963
14	J. Dunham	The pressure distribution round a lifting circular cylinder. Unpublished M.O.A. Report.

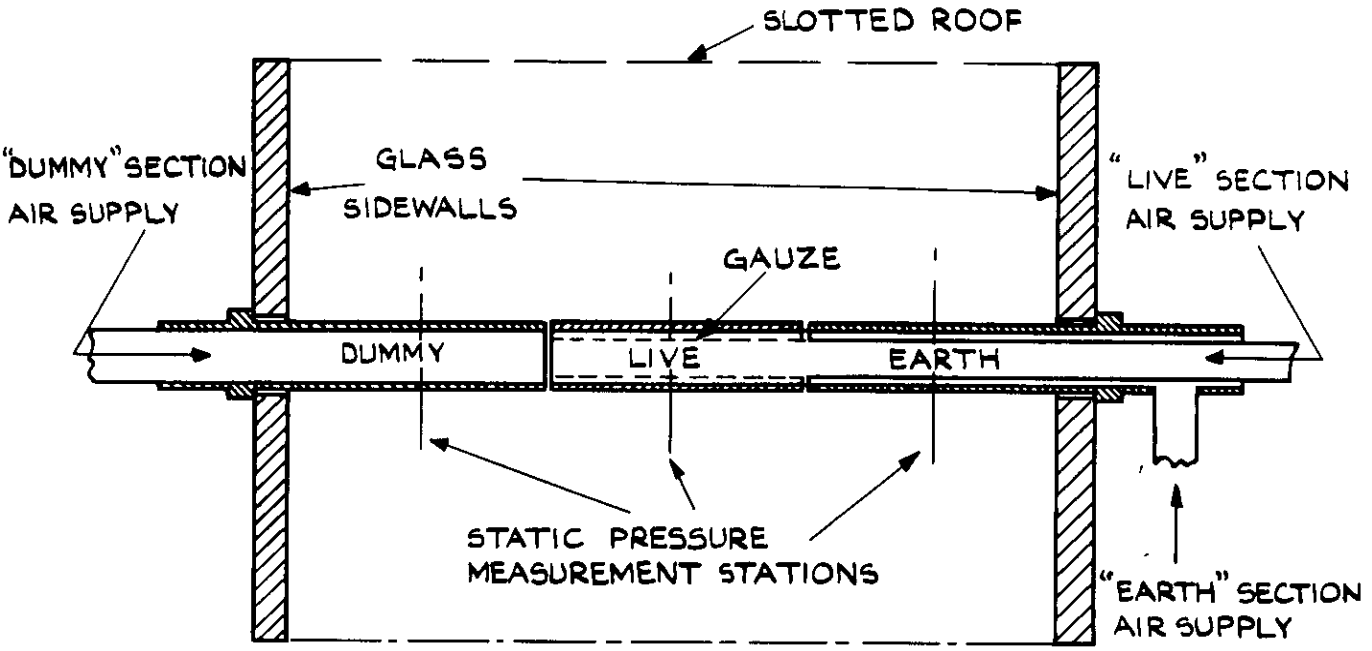

GENERAL ARRANGEMENT OF MODEL.

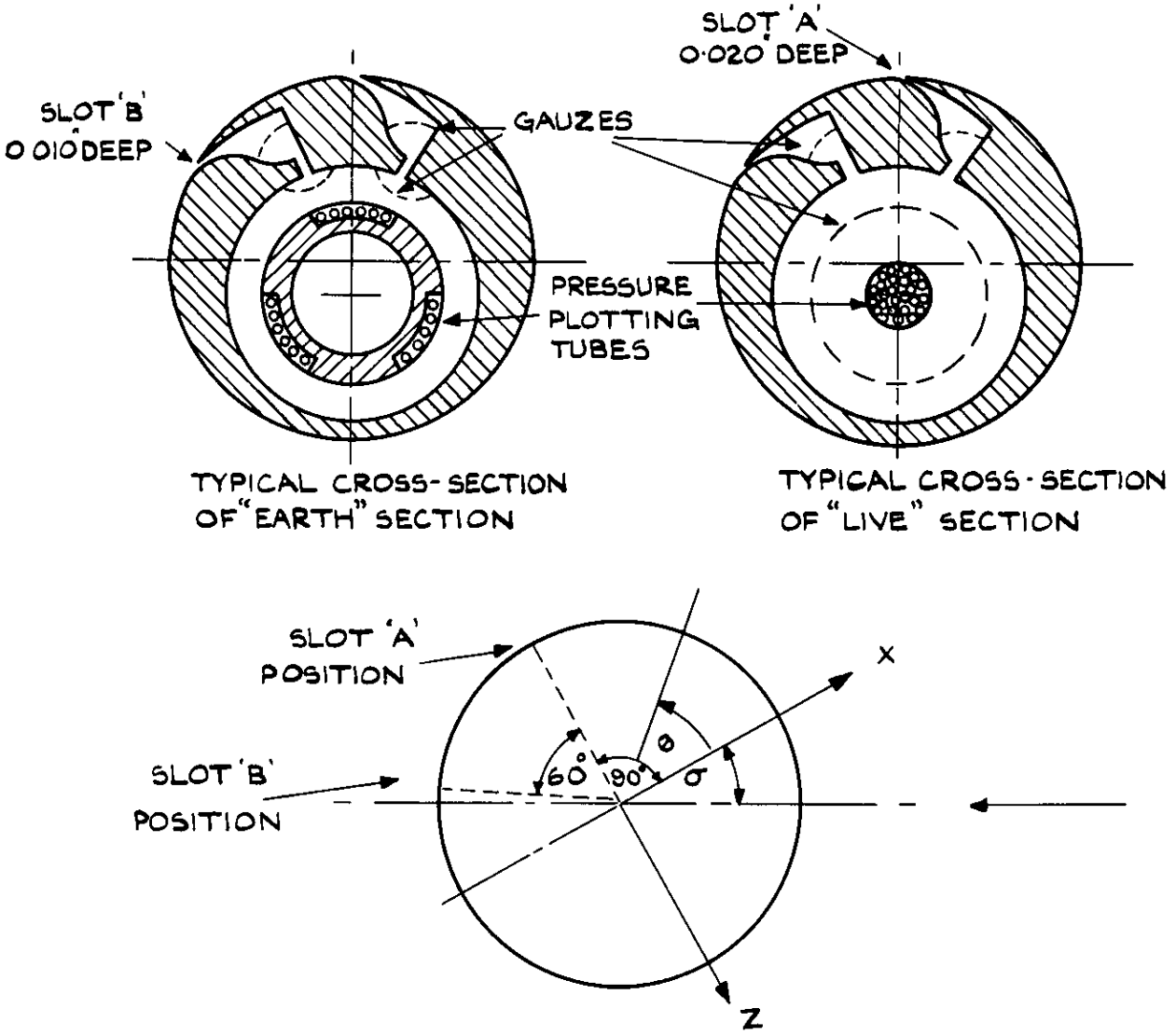

FIG. 1 (a) MODEL GEOMETRY.

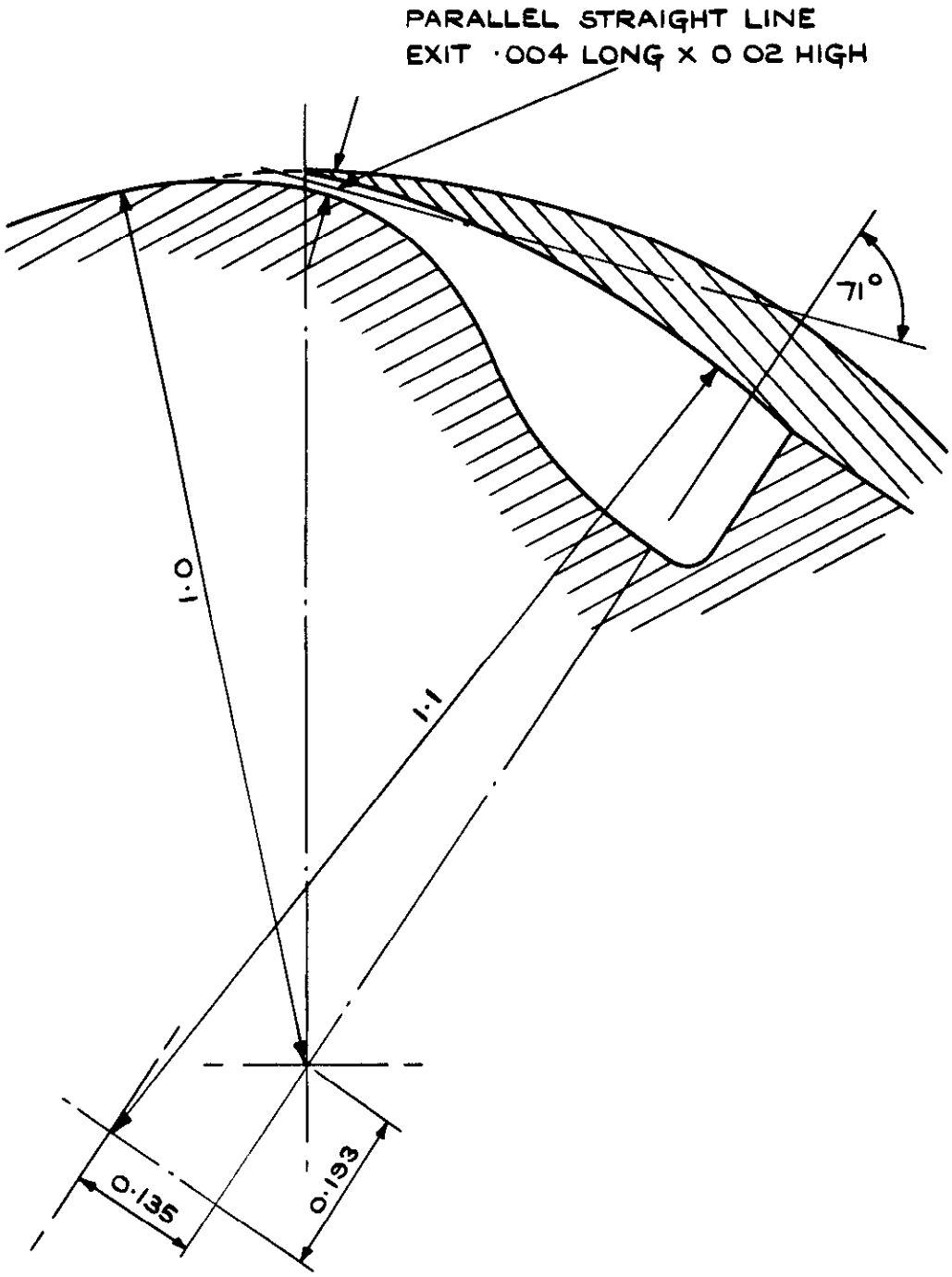

ALL DIMENSIONS IN INCHES

FIG. 1 (b) SLOT GEOMETRY – SLOT A

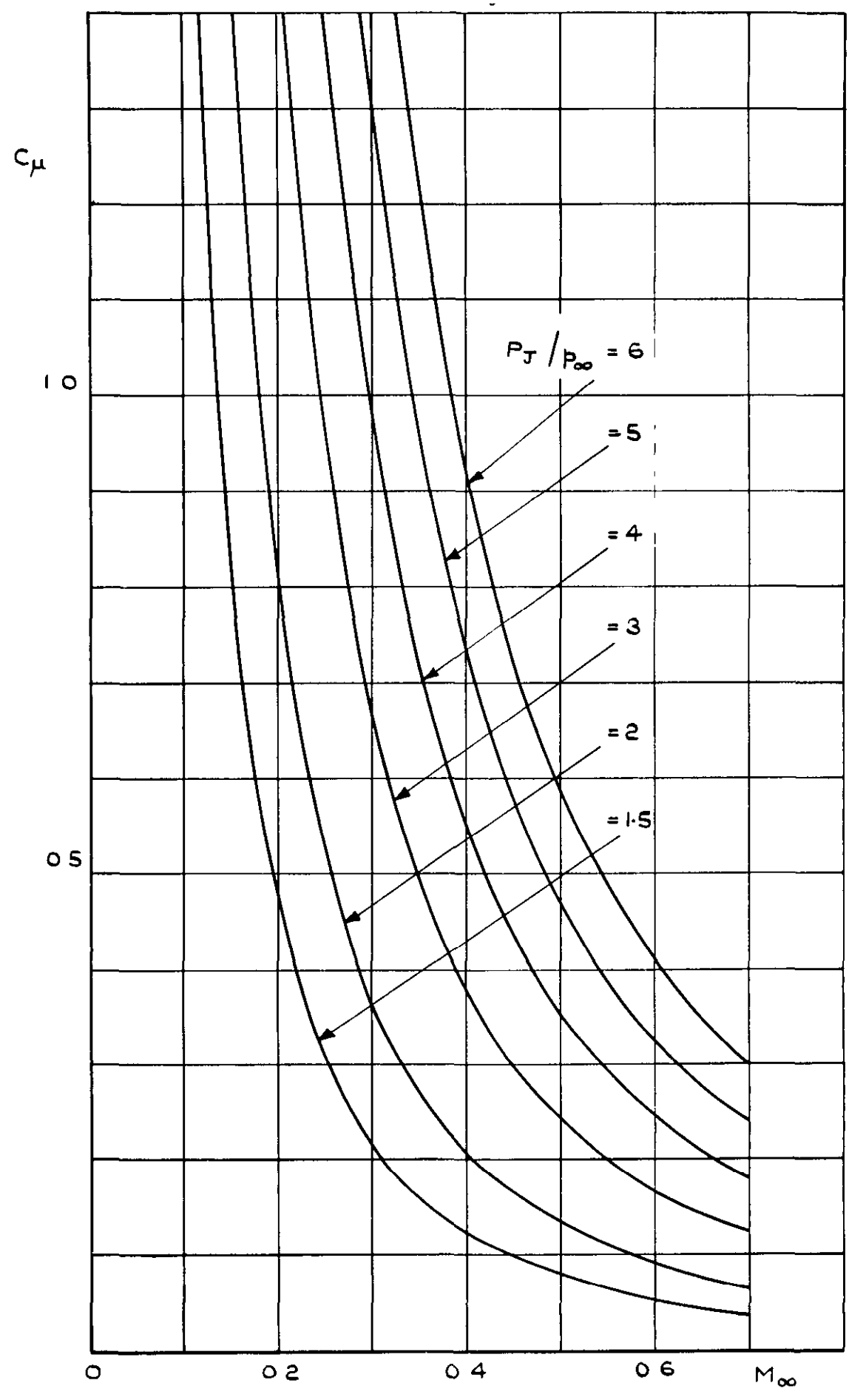

FIG.2 EFFECT OF MACH NUMBER ON $C\mu$ FOR THE PRESENT SLOT GEOMETRY AT CONSTANT P_J/p_∞ (WITH $P_{J_2} = P_{J_1}$)

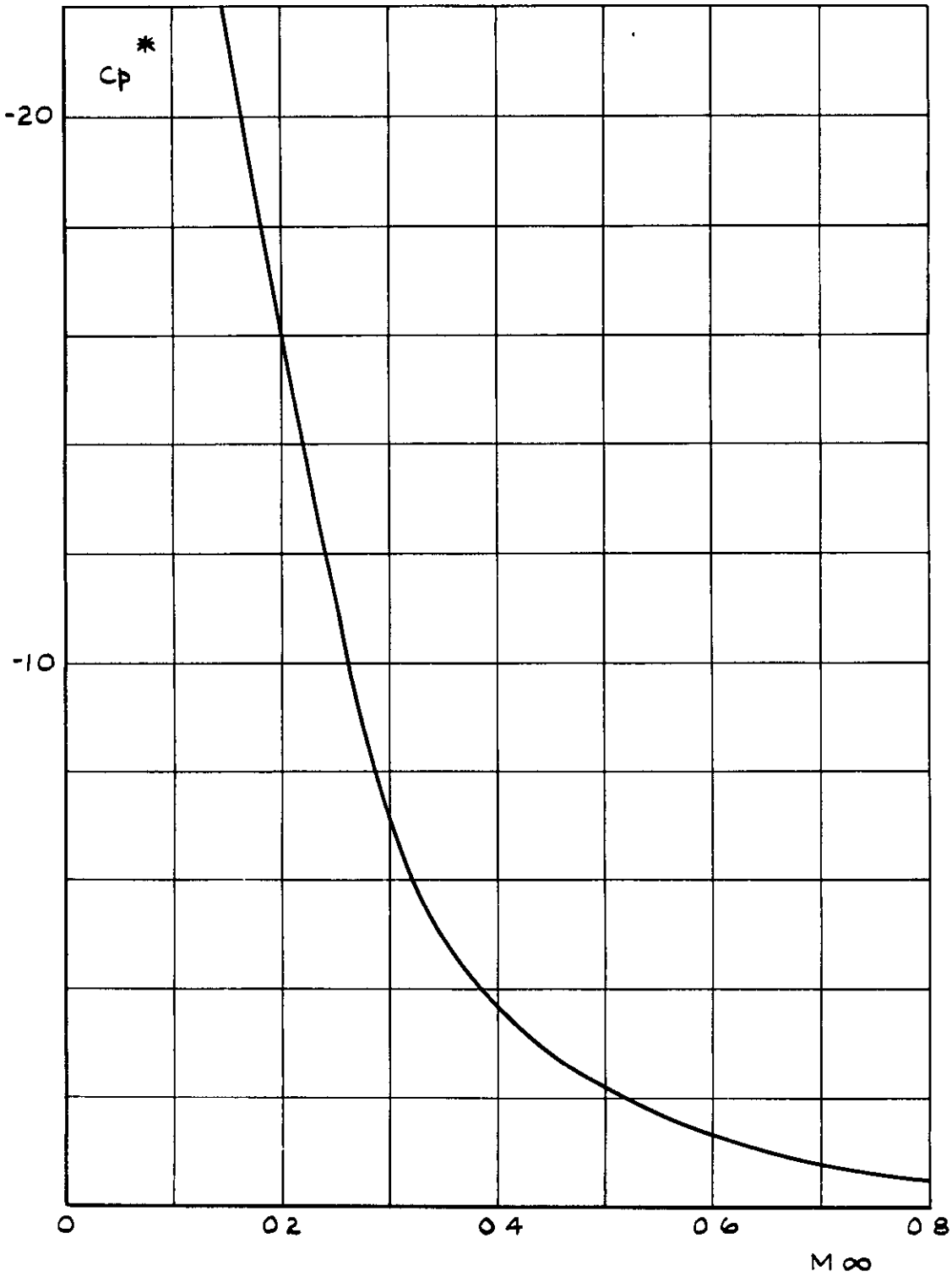

FIG. 3 PRESSURE COEFFICIENT FOR LOCAL SONIC FLOW VERSUS MACH NUMBER

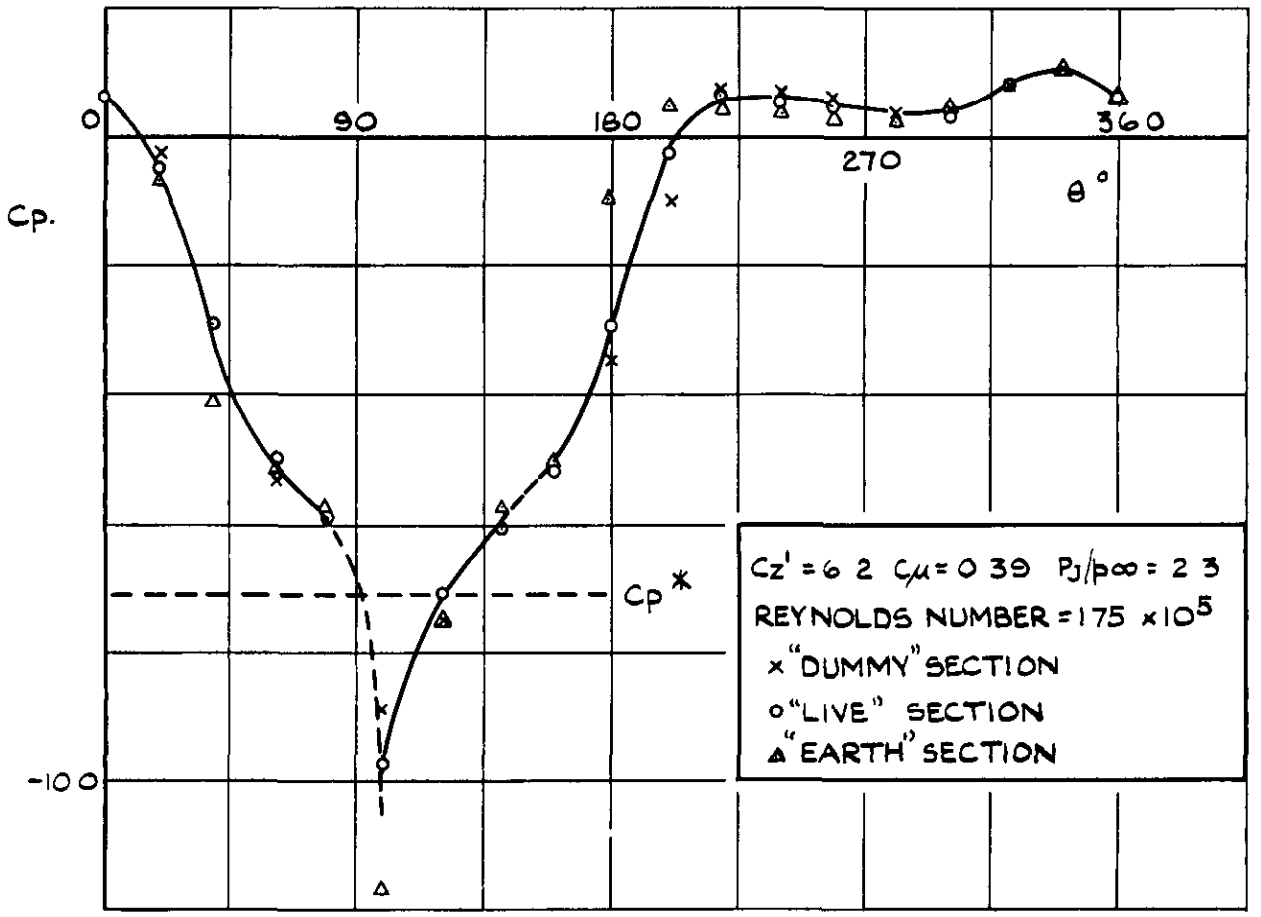

FIG. 4 TYPICAL VARIATION OF Cp WITH θ AT DIFFERENT SPANWISE STATIONS – M∞ = 0·3

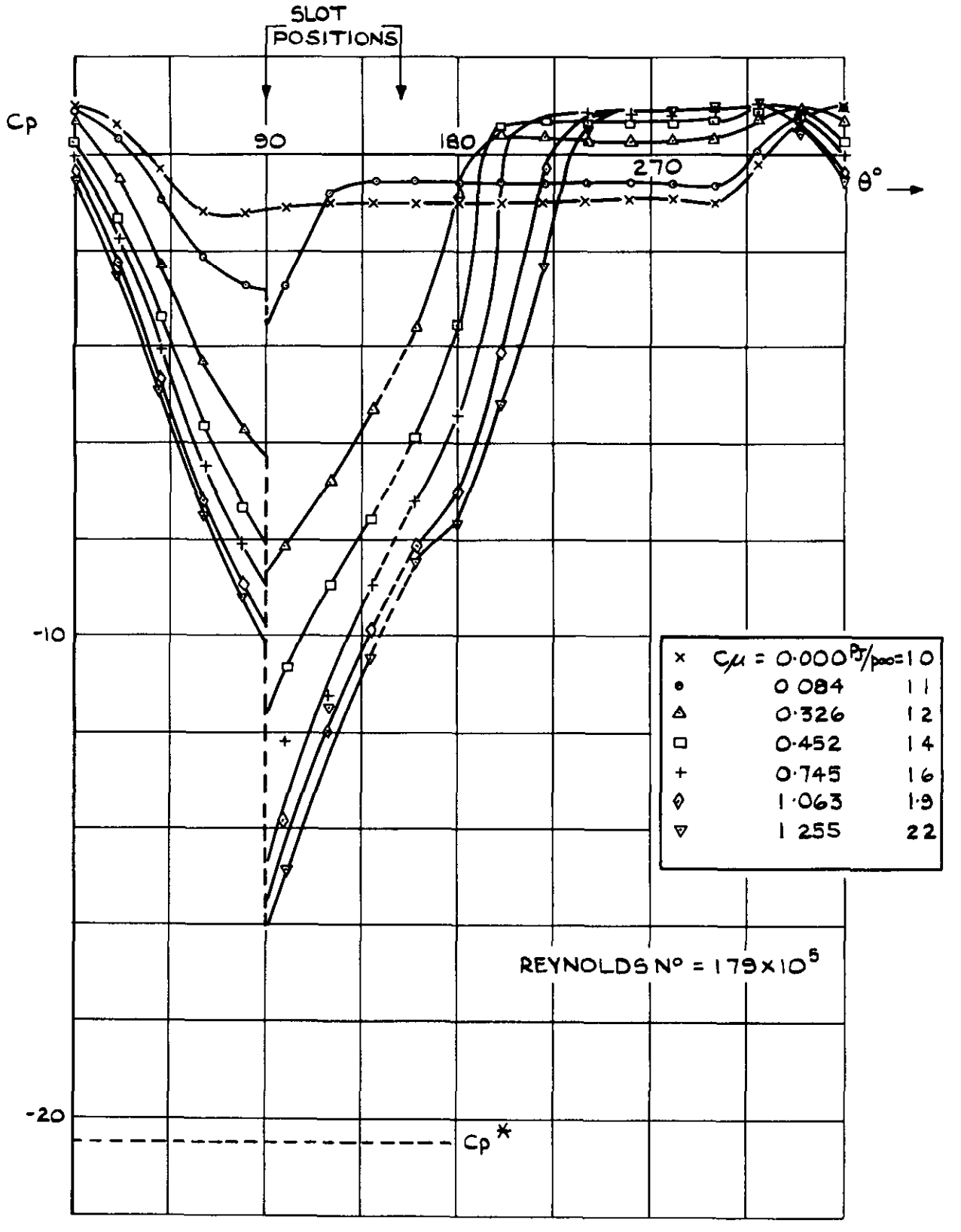

FIG. 5 PRESSURE DISTRIBUTIONS AT MACH NUMBER=0 16.

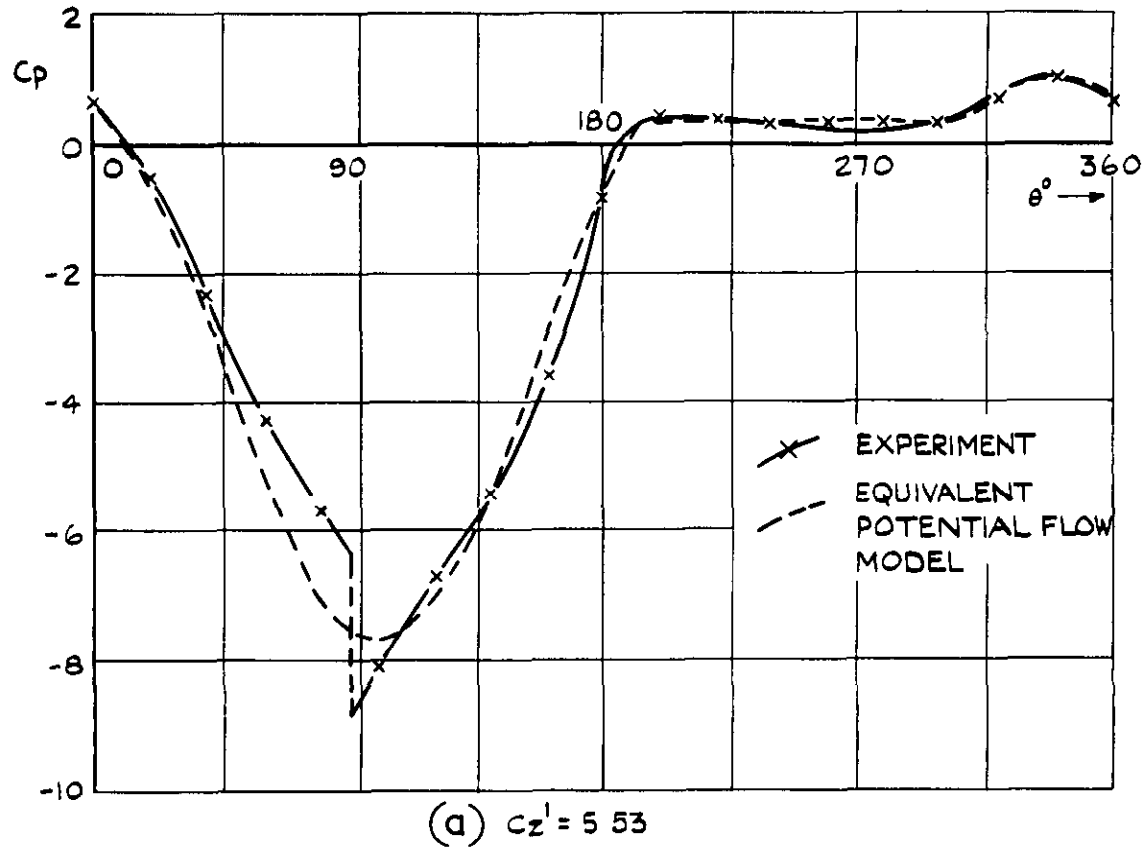

(a) $C_z' = 5\ 53$

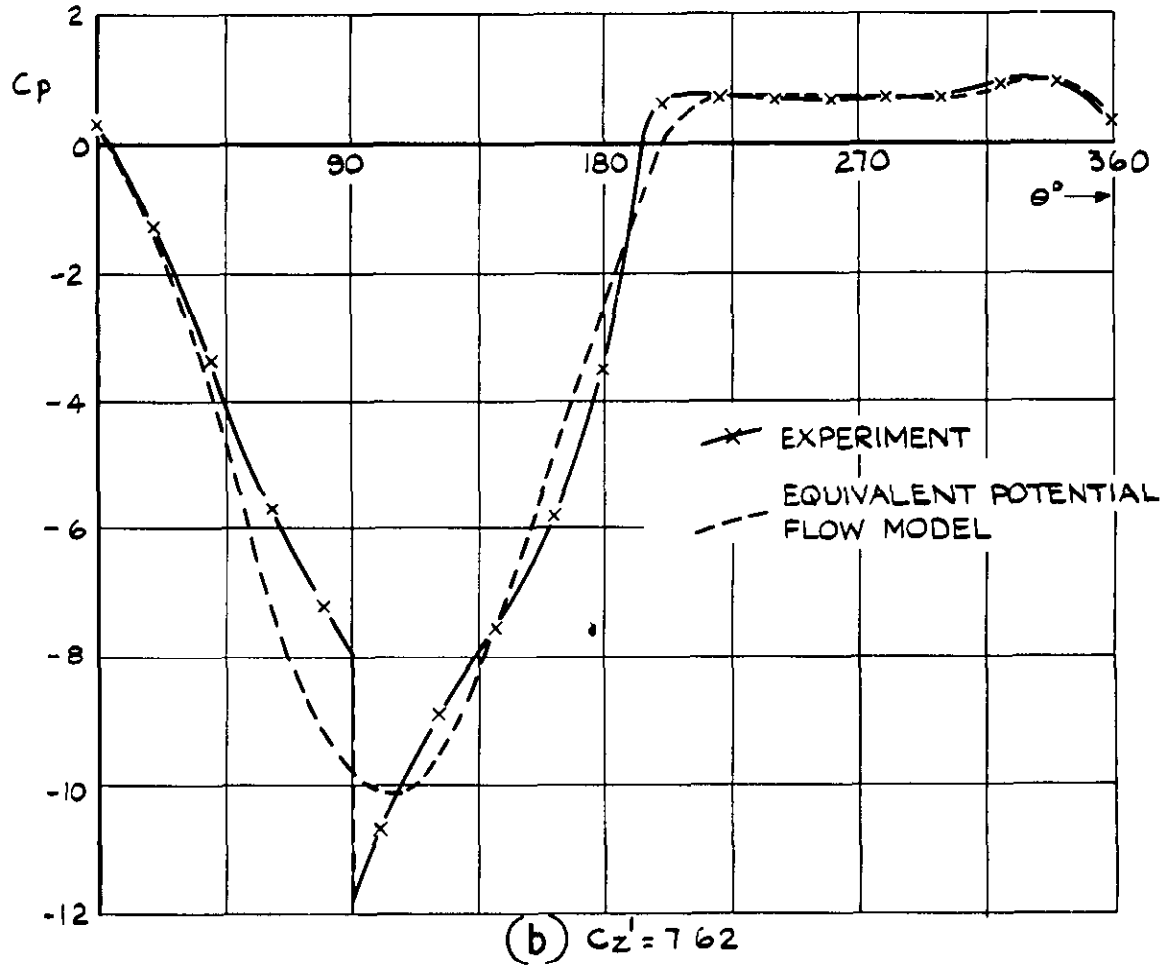

(b) $C_z' = 7\ 62$

FIG. 6 PRESSURE DISTRIBUTIONS AT $M_\infty = 0{\cdot}16$ COMPARED WITH SEMI-EMPIRICAL THEORY OF REFERENCE (14).

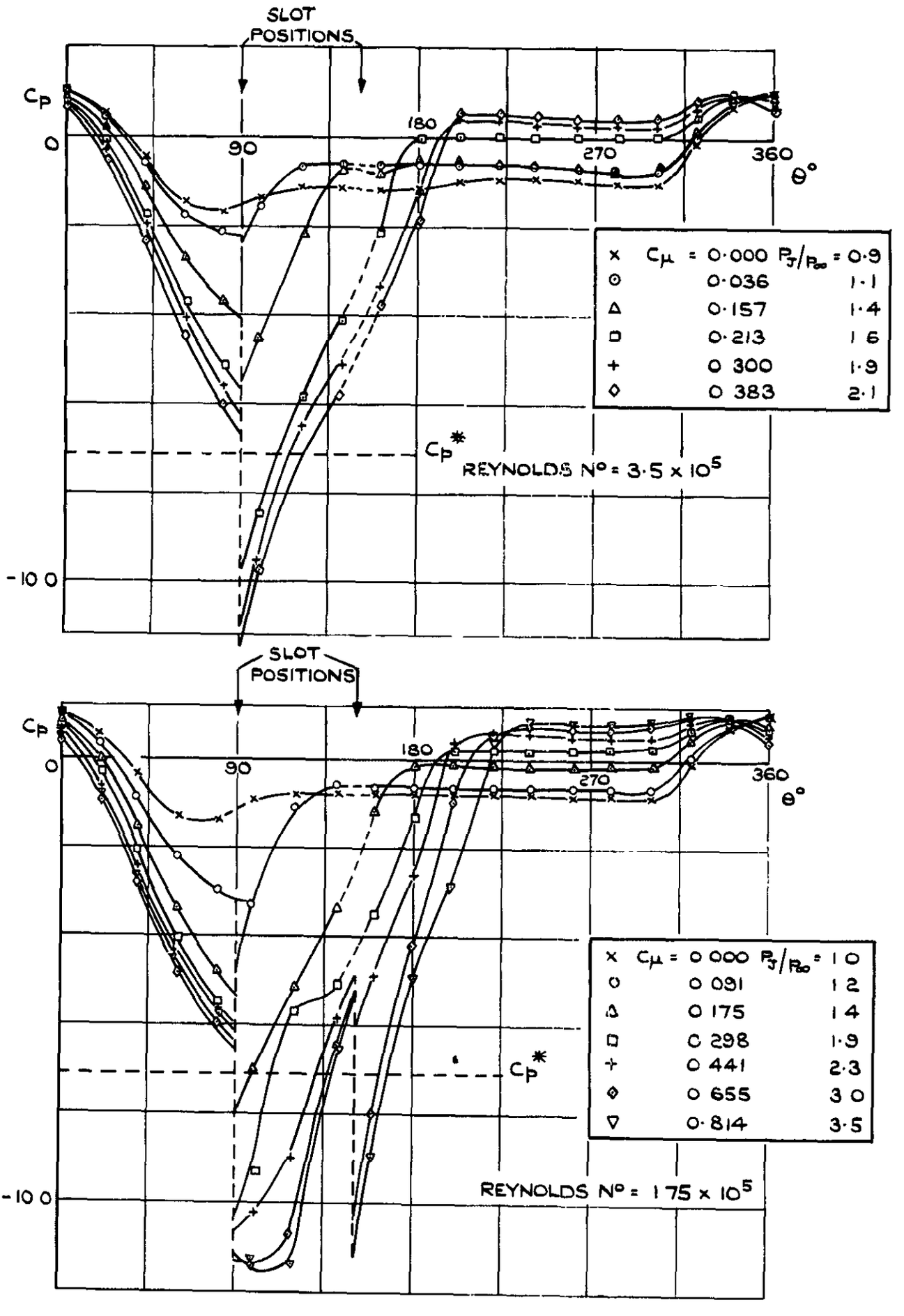

FIG.7 PRESSURE DISTRIBUTIONS AT MACH NUMBER = 0·3

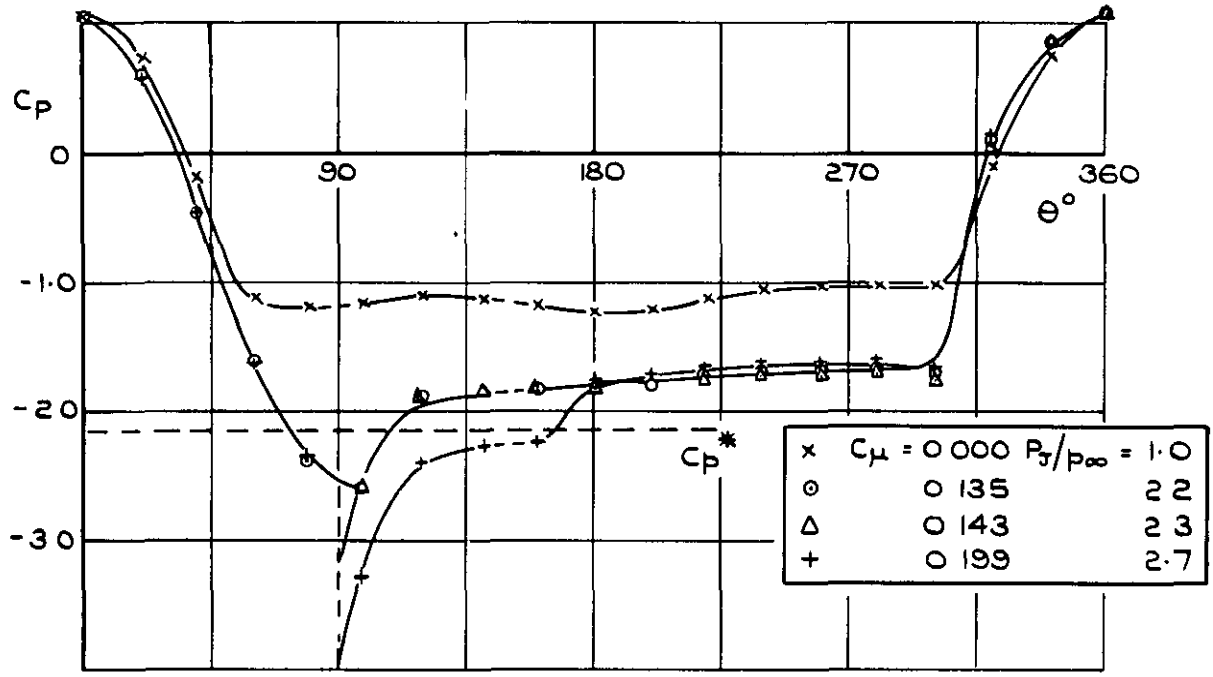

(a) MACH NUMBER = 0·5 (R_e = 1·8 x 10^5)

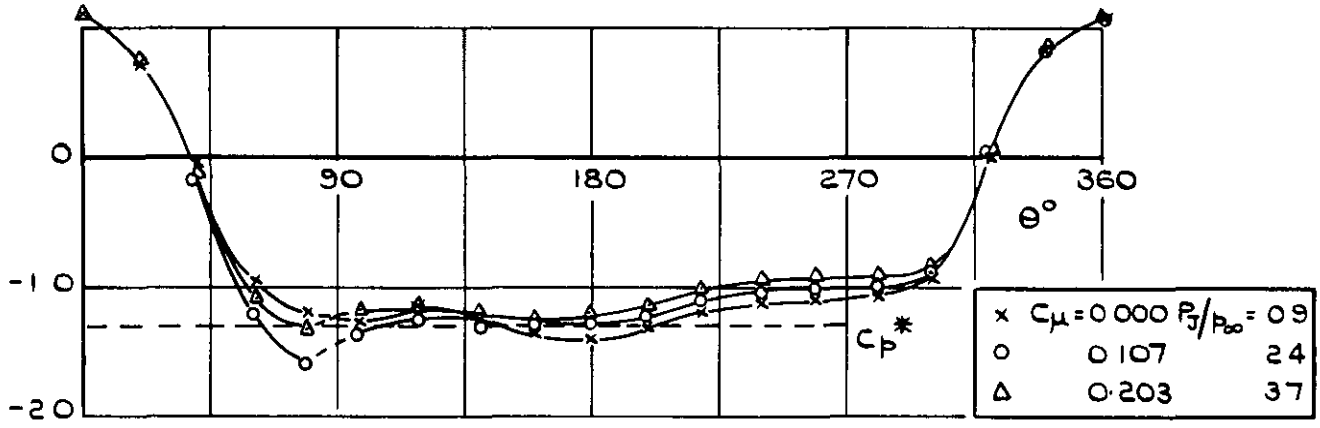

(b) MACH NUMBER = 0·6 (R_e = 1·8 x 10^5)

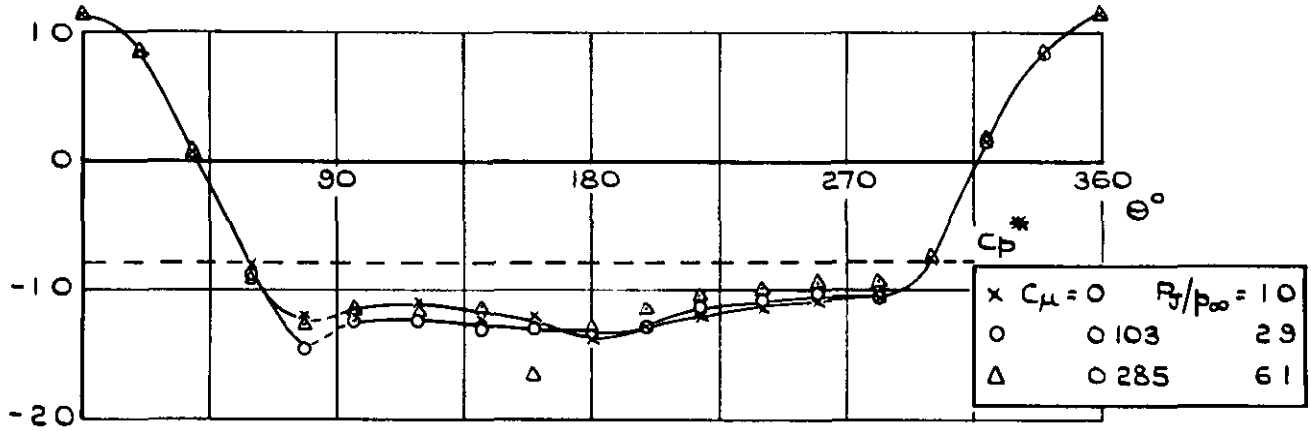

(c) MACH NUMBER = 0·7 (R_e = 1 8 x 10^5)

FIG 8 STATIC PRESSURE DISTRIBUTIONS AT VARIOUS MACH NUMBERS

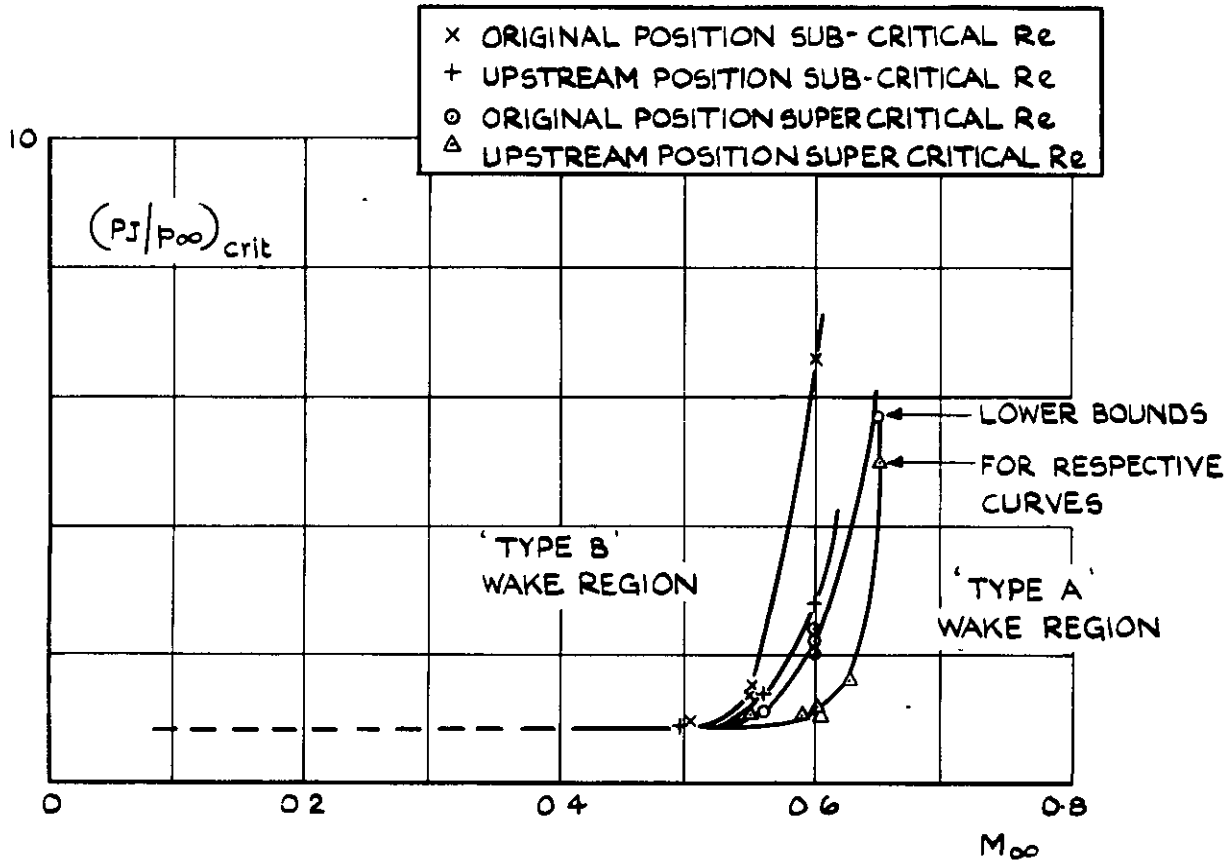

FIG.9 JET PRESSURE RATIO FOR CHANGE IN WAKE CONFIGURATION AGAINST MACH NUMBER

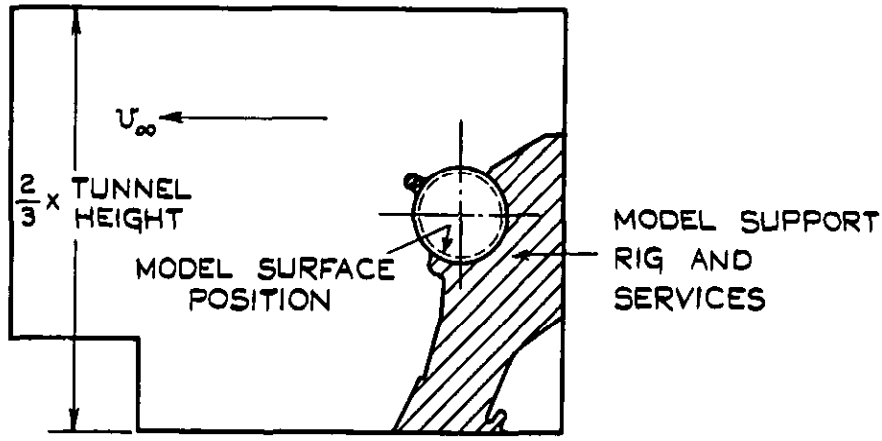

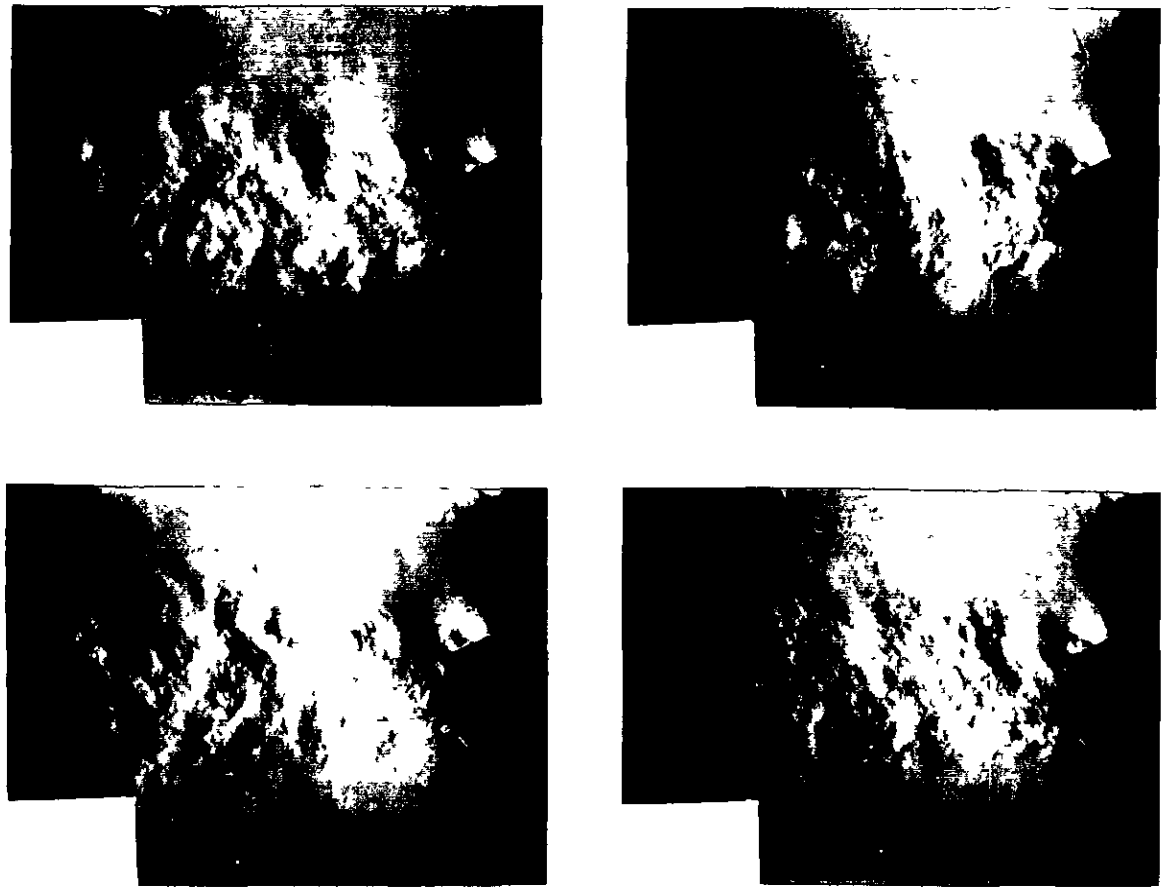

Fig 10a. Spark schlieren photographs of wake "type B" case M_∞=0 50

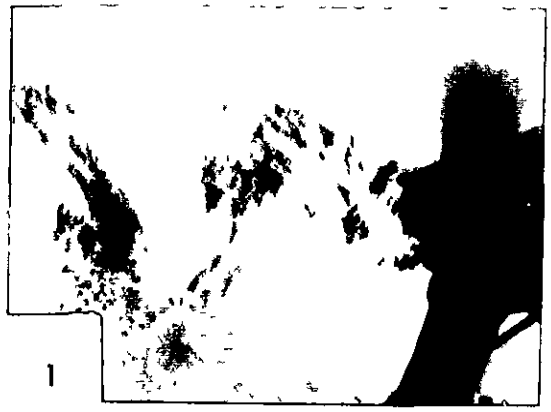

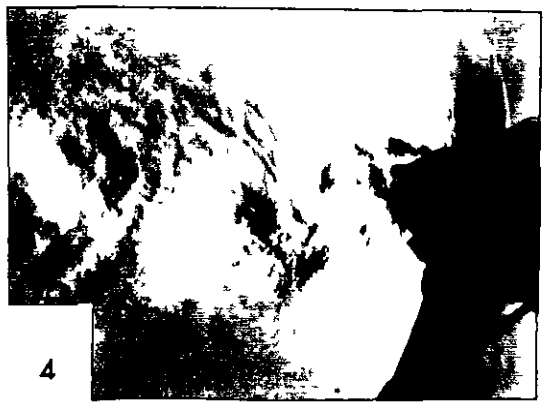

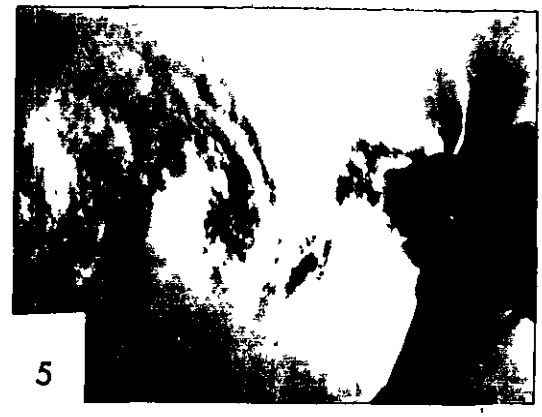

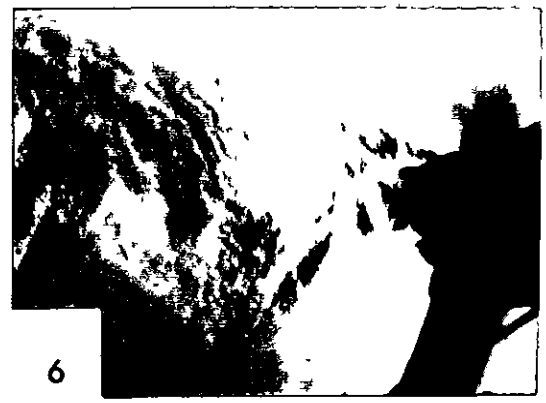

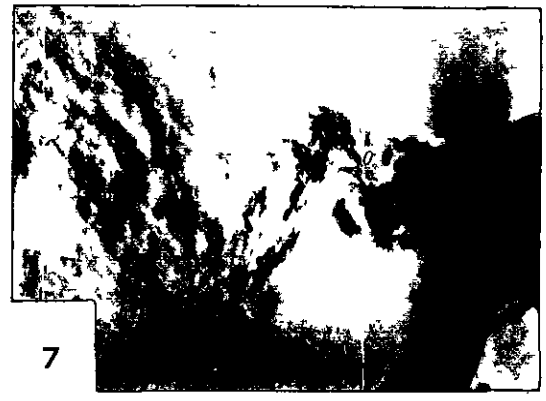

Fig.10b.
Spark schlieren photographs of wake "type A" case $M_{\infty}=0.55$

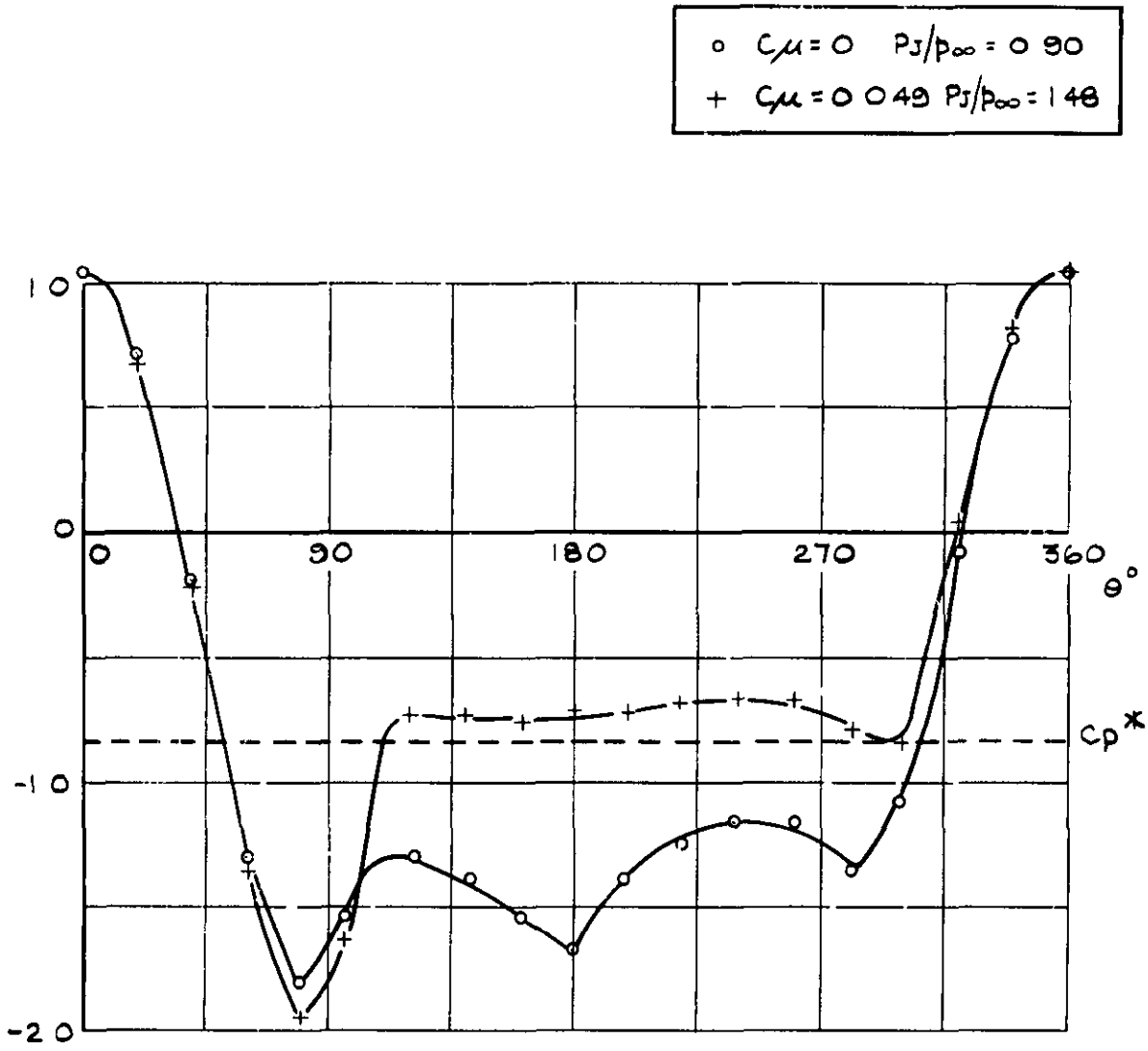

FIG. 11 MEAN STATIC PRESSURE DISTRIBUTIONS AT $M_\infty = 0.55$ CLOSE TO THE WAKE TRANSITION POINT

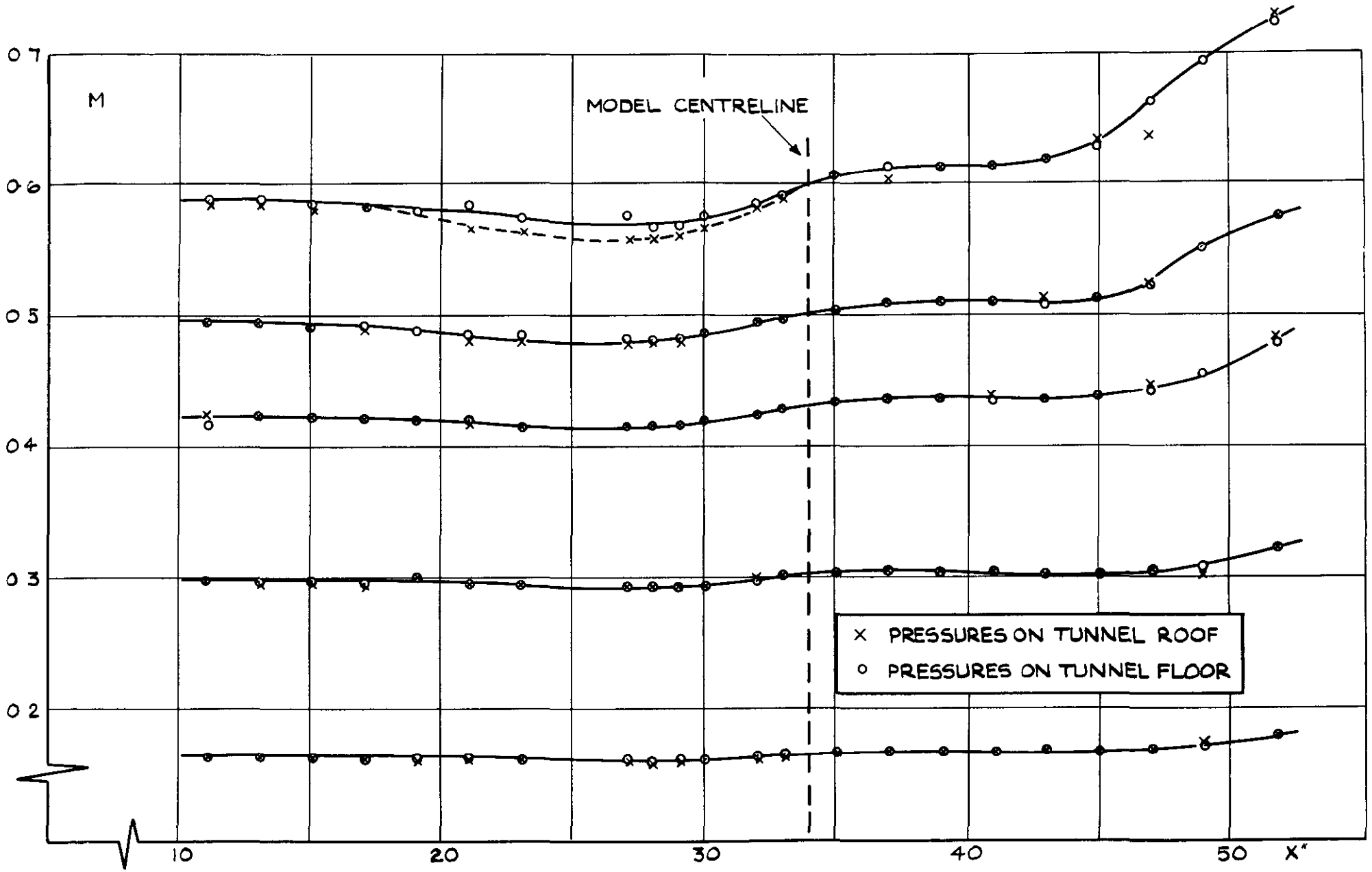

FIG.12 MACH NUMBER DISTRIBUTION DERIVED FROM ROOF & FLOOR STATIC PRESSURE DISTRIBUTONS - ORIGINAL MODEL POSITION AT $C_\mu = 0$.

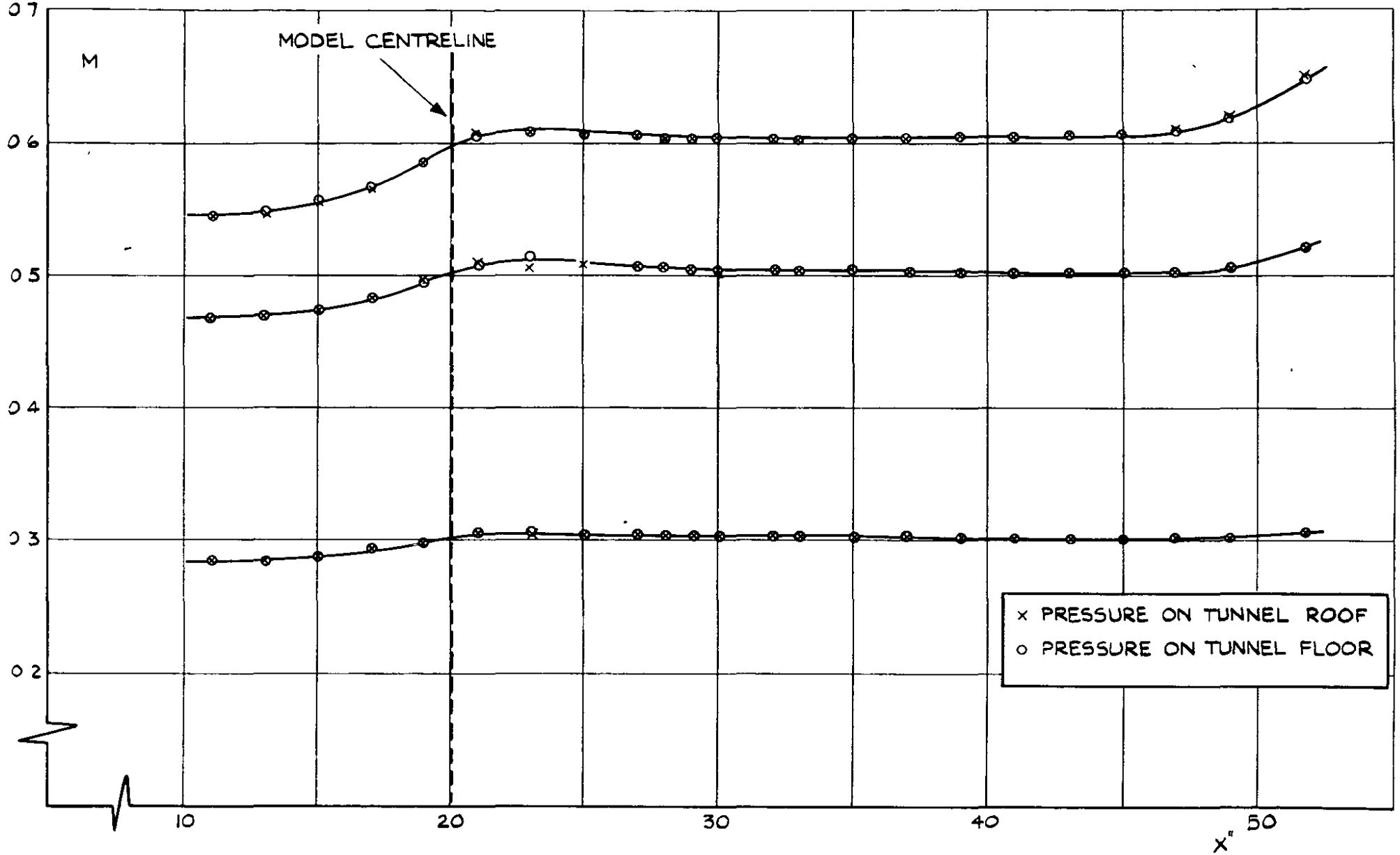

FIG 13 MACH NUMBER DISTRIBUTION DERIVED FROM ROOF & FLOOR STATIC PRESSURE DISTRIBUTION – UPSTREAM MODEL POSITION AT $C_\mu = 0$

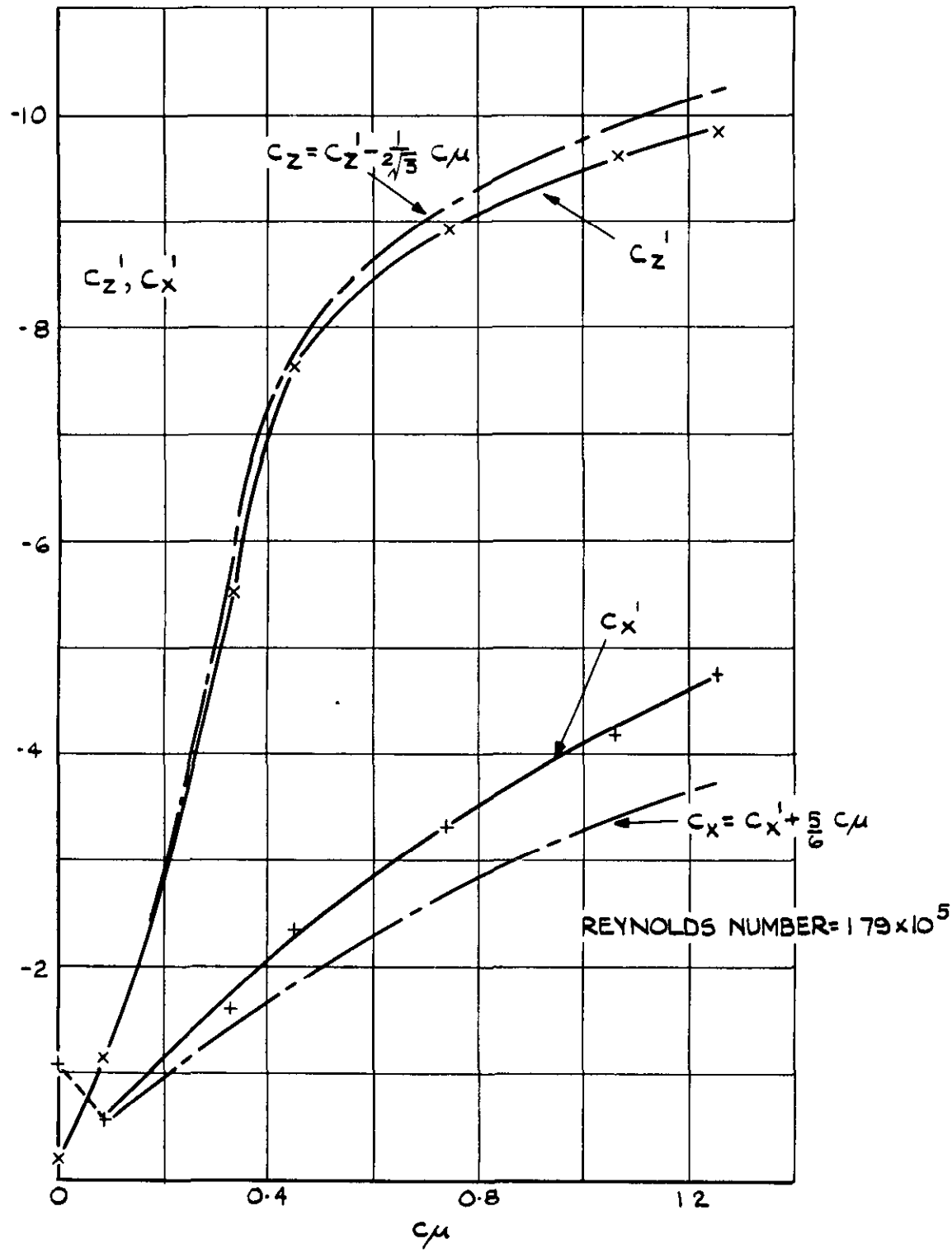

FIG.14 C_z' AND C_x' VERSUS C_μ AT $M_\infty = 0{\cdot}16$

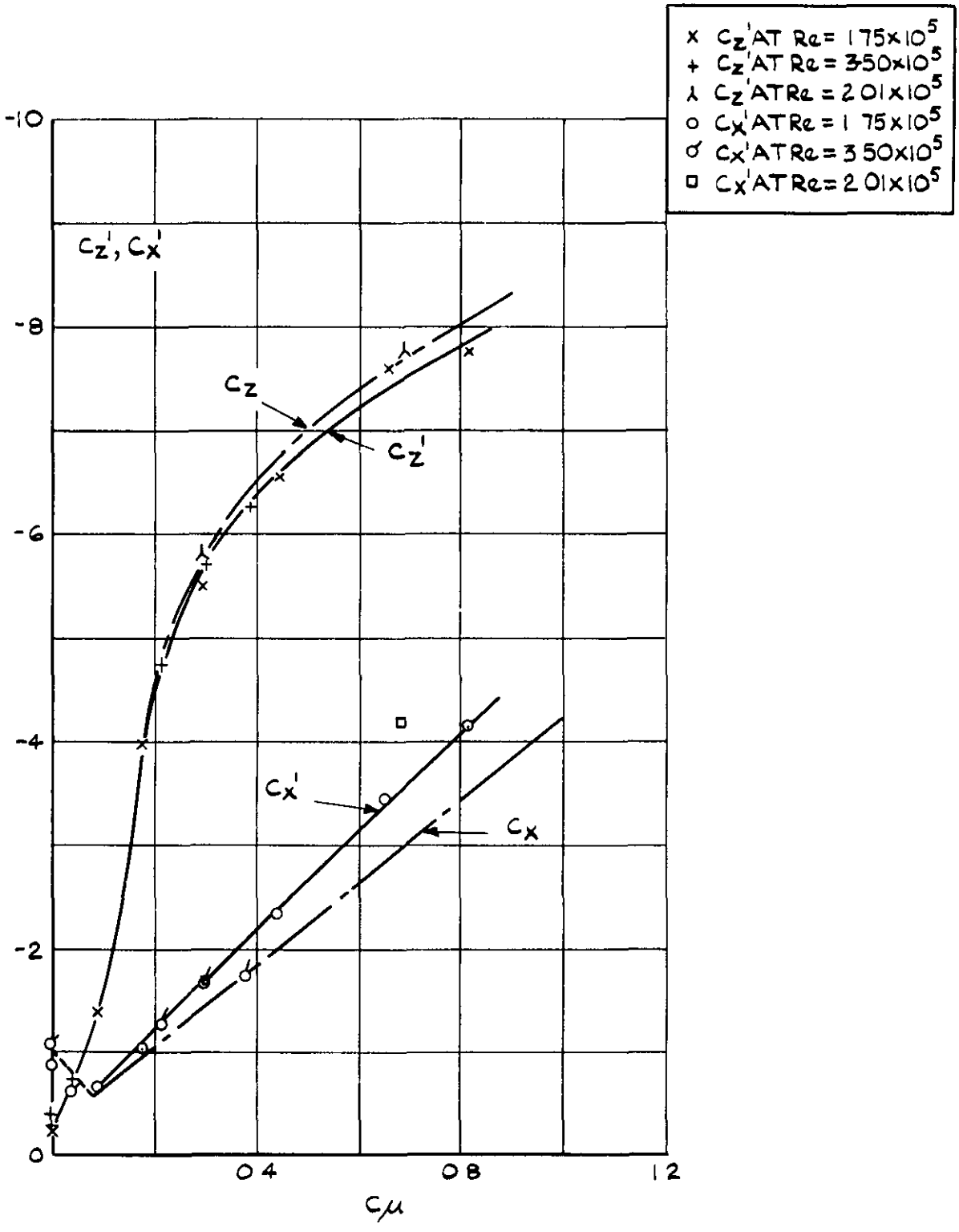

FIG 15 C_z' AND C_x' VERSUS C_μ AT $M_\infty = 0.30$

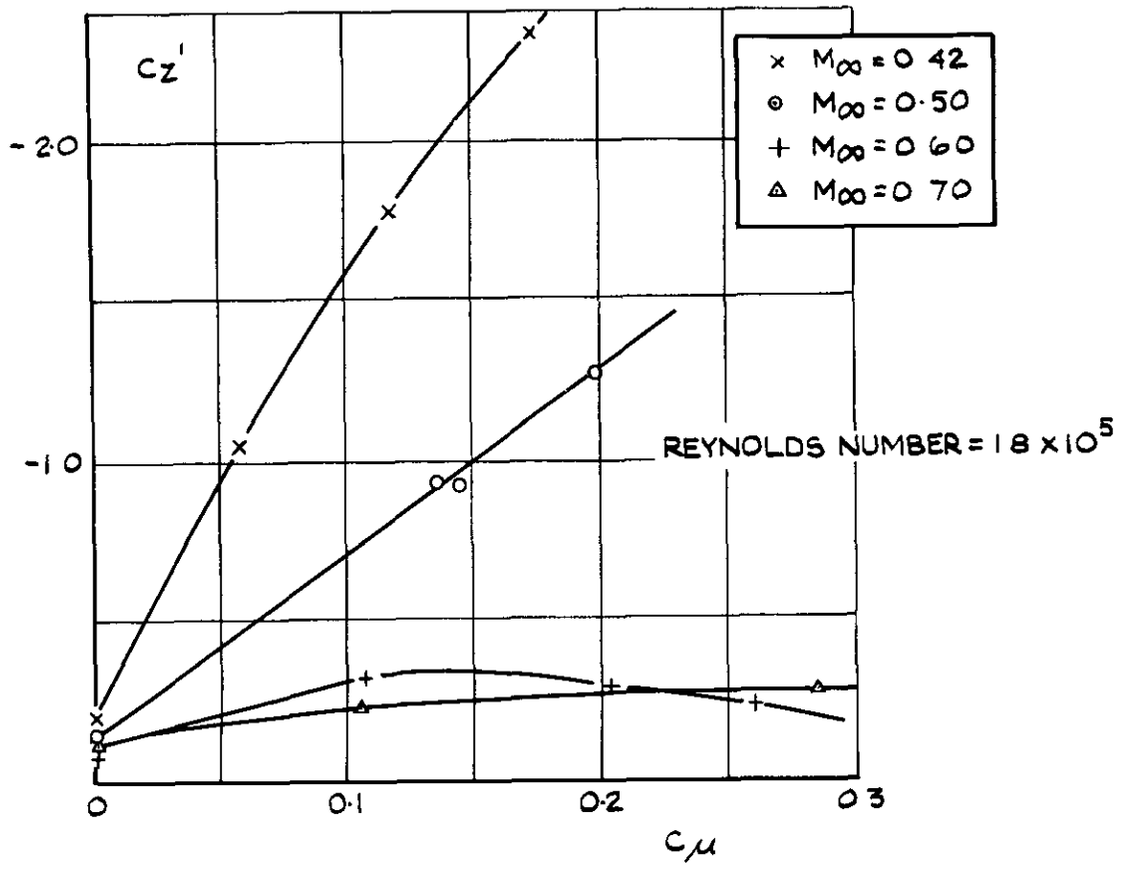

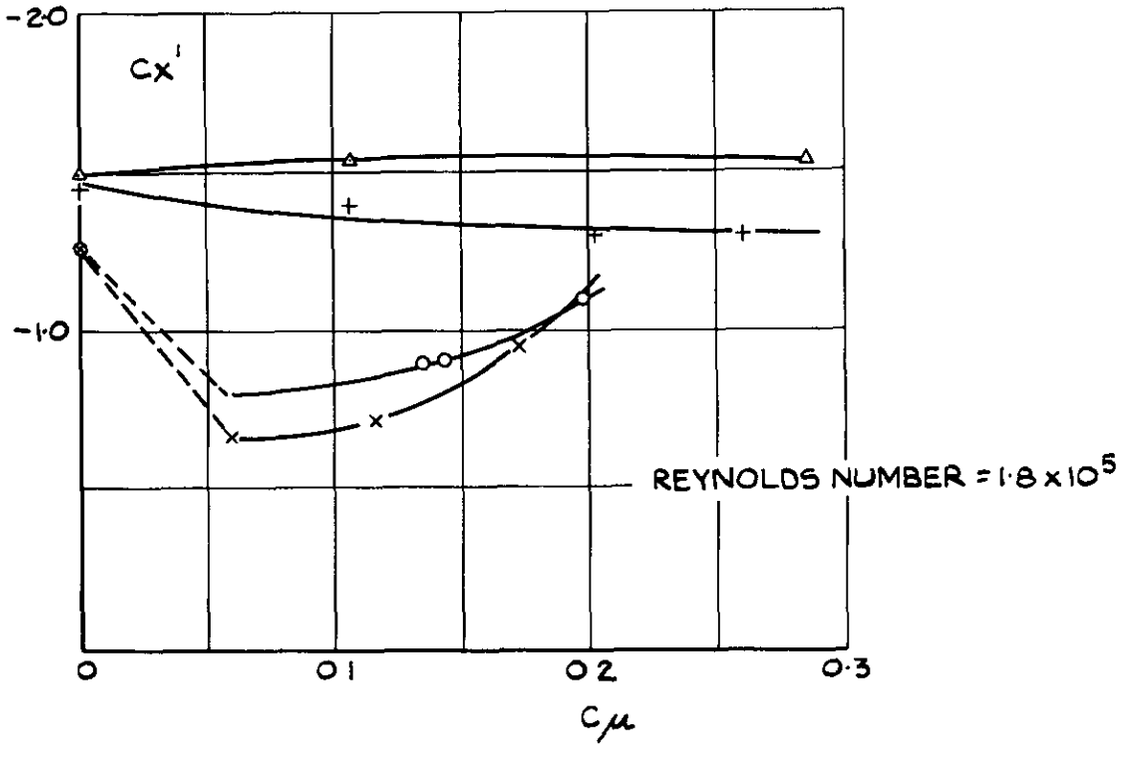

FIG.16 C_z' AND C_x' VERSUS C_μ AT VARIOUS MACH NUMBERS.

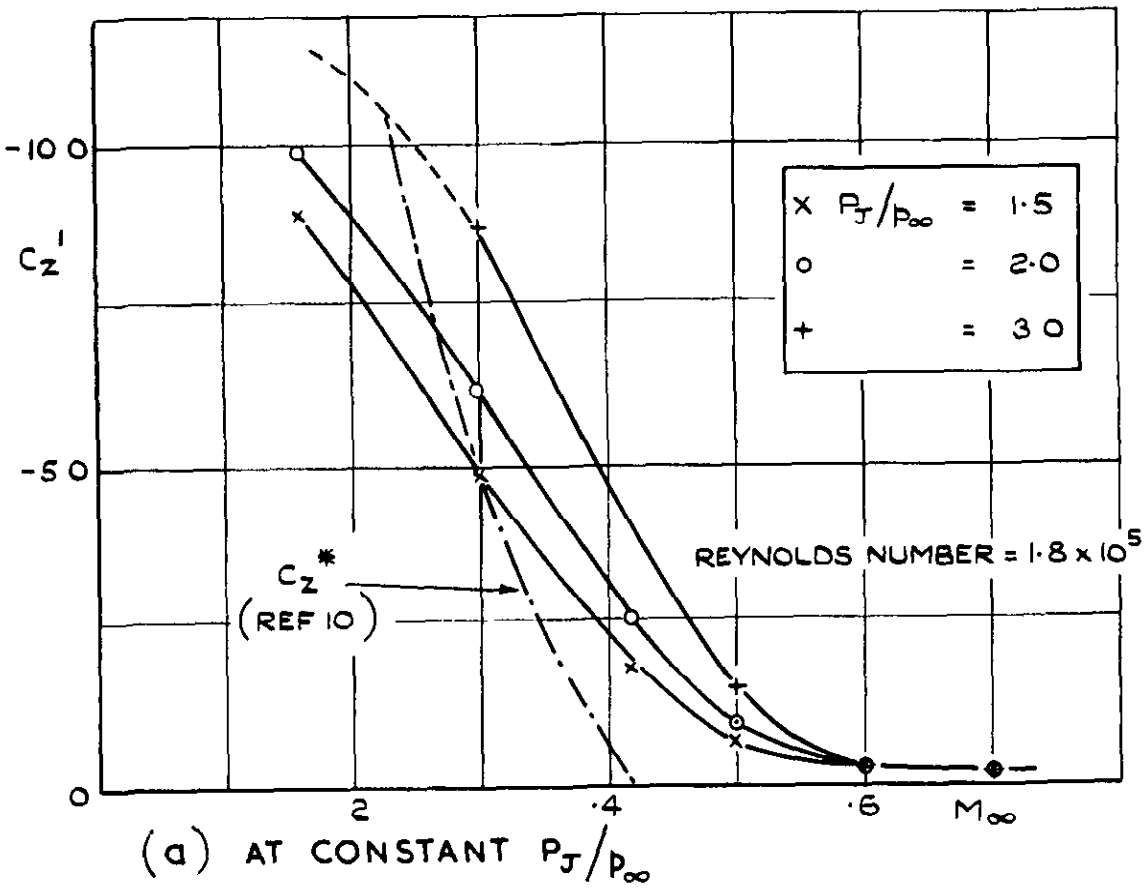

(a) AT CONSTANT P_J/p_∞

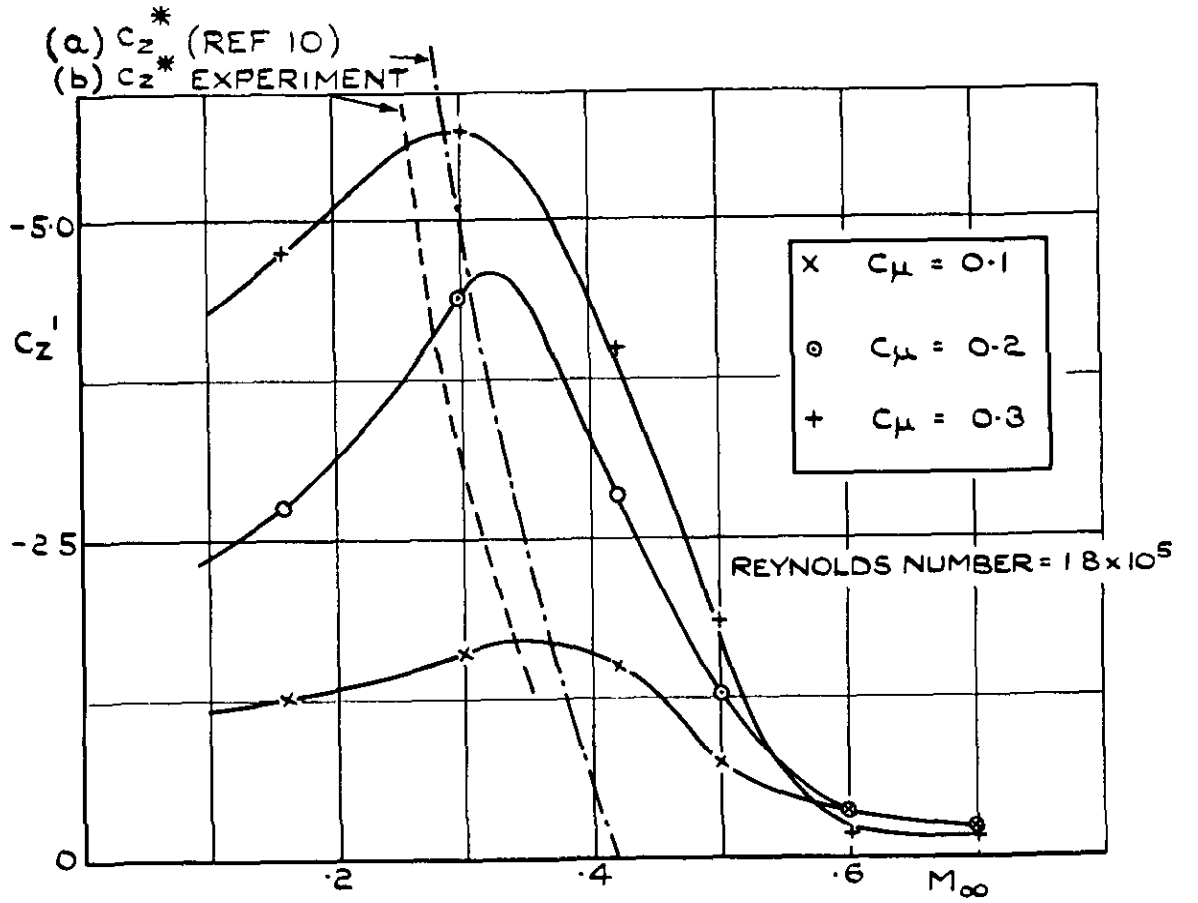

(b) AT CONSTANT C_μ

FIG.17 EFFECT OF MACH No ON NORMAL FORCE CHARACTERISTICS

Printed in England for Her Majesty's Stationery Office by the Royal Aircraft Establishment, Farnborough. Dd.125875. K.5.

A.R.C. CP No. 889

December 1964

A. F. Jones
W. R. Buckingham

533.696.3: 533.694.2:
533.6.011.7: 533.6.048.2:
533.6.011.32

SOME EXPLORATORY TESTS ON A TWO-DIMENSIONAL BLOWN-CYLINDER MODEL IN THE R.A.E. 2 FT x 1½ FT TRANSONIC WIND TUNNEL

Static pressure measurements have been made at subsonic Mach numbers to examine compressibility effects on a two-dimensional circular cylinder with two tangential blowing slots. These results together with forces derived from them are briefly discussed.

A.R.C. CP No. 889

December 1964

A. F. Jones
W. R. Buckingham

533.696.3: 533.694.2:
533.6.011.7: 533.6.048.2:
533.6.011.32

SOME EXPLORATORY TESTS ON A TWO-DIMENSIONAL BLOWN-CYLINDER MODEL IN THE R.A.E. 2 FT x 1½ FT TRANSONIC WIND TUNNEL

Static pressure measurements have been made at subsonic Mach numbers to examine compressibility effects on a two-dimensional circular cylinder with two tangential blowing slots. These results together with forces derived from them are briefly discussed.

A.R.C. CP No. 889

December 1964

A. F. Jones
W. R. Buckingham

533.696.3: 533.694.2:
533.6.011.7: 533.6.048.2:
533.6.011.32

SOME EXPLORATORY TESTS ON A TWO-DIMENSIONAL BLOWN-CYLINDER MODEL IN THE R.A.E. 2 FT x 1½ FT TRANSONIC WIND TUNNEL

Static pressure measurements have been made at subsonic Mach numbers to examine compressibility effects on a two-dimensional circular cylinder with two tangential blowing slots. These results together with forces derived from them are briefly discussed.

Published by
HER MAJESTY'S STATIONERY OFFICE

To be purchased from
49 High Holborn, London W.C.1
423 Oxford Street, London W.1
13A Castle Street, Edinburgh 2
109 St Mary Street, Cardiff
Brazennose Street, Manchester 2
50 Fairfax Street, Bristol 1
35 Smallbrook, Ringway, Birmingham 5
80 Chichester Street, Belfast 1
or through any bookseller

C.P. No. 889

S.O. CODE No. 23-9016-89